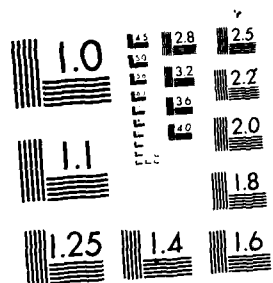


AD-A173 851 ANALYSIS OF THE VIBRATION OF THE INPUT BEVEL PINION IN 1/1
RAN (ROYAL AUSTRALIAN) AERONAUTICAL RESEARCH LABS
MELBOURNE (AUSTRALIA) P D MCFADDEN SEP 85
UNCLASSIFIED ARL-AERO-PROP-A-169 F/G 1/3 NL

END
DATE
FILMED
12-86



MICROCOPY RESOLUTION TEST CHART
NATIONAL BUREAU OF STANDARDS-1963-A

12

AD-A173 851

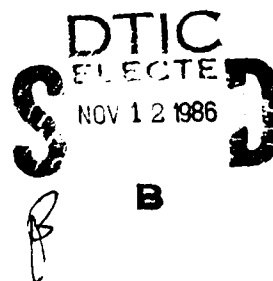


DEPARTMENT OF DEFENCE
DEFENCE SCIENCE AND TECHNOLOGY ORGANISATION
AERONAUTICAL RESEARCH LABORATORIES
MELBOURNE, VICTORIA

AERO PROPULSION REPORT 169

**ANALYSIS OF THE VIBRATION OF THE INPUT BEVEL
PINION IN RAN WESSEX HELICOPTER MAIN ROTOR
GEARBOX WAK143 PRIOR TO FAILURE**

by
P. D. McFADDEN



DTIC FILE COPY

Approved for public release.

THE UNITED STATES NATIONAL
TECHNICAL INFORMATION SERVICE
IS AUTHORISED TO
REPRODUCE AND SELL THIS REPORT

© COMMONWEALTH OF AUSTRALIA 1985

COPY No

SEPTEMBER 1985

86 11 12 003

AR-004-049

DEPARTMENT OF DEFENCE
DEFENCE SCIENCE AND TECHNOLOGY ORGANISATION
AERONAUTICAL RESEARCH LABORATORIES

AERO PROPULSION REPORT 169

**ANALYSIS OF THE VIBRATION OF THE INPUT BEVEL
PINION IN RAN WESSEX HELICOPTER MAIN ROTOR
GEARBOX WAK143 PRIOR TO FAILURE**

by
P. D. McFADDEN

DTIC
ELECTE
NOV 12 1986
B

SUMMARY

Following the crash of an RAN Wessex helicopter caused by the catastrophic fatigue failure of the input spiral bevel pinion in the main rotor gearbox, routine recordings of the gearbox vibration have been analyzed by ARL. It has been shown that conventional spectral analysis of the vibration is unable to give adequate indication of the presence of the fatigue crack but that an alternative technique of vibration analysis called signal averaging can give warning of the crack 42 hours before failure. Enhancement of the signal average using a computer enables detection of the crack as early as 103 hours before failure.



© COMMONWEALTH OF AUSTRALIA (1985)

POSTAL ADDRESS: Director, Aeronautical Research Laboratories,
Box 4331, Melbourne, Victoria, 3001, Australia.

CONTENTS

Section	Page No.
1. INTRODUCTION	1
2. SPECTRAL ANALYSIS OF GEAR VIBRATION	2
2.1 Introduction	2
2.2 Weighting Functions	2
2.3 Spectrum of WAK143	3
3. SIGNAL AVERAGING OF GEAR VIBRATION	4
3.1 Introduction	4
3.2 Calculating the Signal Average	4
3.3 Frequency Multiplication	5
3.4 Computer Implementation	7
3.5 Signal Average of WAK143	7
4. ENHANCEMENT OF THE SIGNAL AVERAGE	8
4.1 Introduction	8
4.2 Elimination	8
4.3 Kurtosis	8
4.4 Application	9
4.5 Ghost Component	9
4.6 Conclusions	10
5. NEW TECHNIQUE FOR ENHANCEMENT	10
5.1 Introduction	10
5.2 Development	10
5.3 Application	12
5.4 Other Gearboxes	13
6. DEMODULATION OF THE SIGNAL AVERAGE	13
6.1 Introduction	13
6.2 Development	14
6.3 Application	14

7. EXCITATION OF RESONANCES BY GEAR TOOTH IMPACTS	15
7.1 Introduction	15
7.2 Development	15
7.3 Application	16
7.4 Discussion	17
7.5 Conclusions	18
8. CONCLUSIONS	18
REFERENCES	
APPENDIX	
FIGURES	
DISTRIBUTION	
DOCUMENT CONTROL DATA	

1. INTRODUCTION

In December 1983 a Wessex Mark 31B helicopter of the Royal Australian Navy (RAN) crashed in Bass Strait with the loss of two lives. After recovery of the aircraft from the sea, the cause of the crash was attributed to the catastrophic failure of the input spiral bevel pinion in the main rotor gearbox, serial number WAK143, as shown in Figure 1. Metallurgical investigations by ARL revealed that the pinion failed because of a fatigue crack which started at a subsurface inclusion near the root of one of the teeth. The crack progressed radially into the gear before growing axially fore and aft as shown in Figure 2, probably over a period of several hundred flying hours. When the crack reached the neck of the gear, it changed direction and moved circumferentially around the gear. During this phase, growth was much more rapid, and it is believed that the crack may have travelled around a large part of the gear in as little as 20 minutes until the final overload failure occurred. It is difficult to establish the history of the crack, particularly the total time to failure, due to damage of the fracture surfaces during the last stage of the crack growth. Nevertheless a possible history of the crack growth since the last inspection has been proposed and is shown in Figure 3[1], while estimates of the crack front positions at various times are given in Figure 4[1].

Methods of oil analysis or oil-borne debris detection cannot locate cracks of this kind, simply because no debris are generated during crack propagation. To detect the crack by visual inspection it would be necessary to remove the pinion at intervals much less than the expected time to failure, and the effect on flying operations of these removals would be disruptive. Fortunately vibration analysis offers a potential solution. Since 1977 the RAN has performed routine spectral analysis of the vibration of the main rotor gearboxes in both Wessex and Sea King helicopters to assist with the condition monitoring of these systems. In the Wessex, an accelerometer is fitted to a bolt on the input housing near the large taper roller bearing on the input bevel pinion shaft before each monitoring-flight. Tape recordings of the signal from the accelerometer are made in flight for a range of torque settings. After the flight the recordings are processed using a Hewlett-Packard HP3582A narrow band spectrum analyzer and each spectrum is examined by an experienced operator for changes which could indicate abnormal operation. In the past, brinelled freewheel bearings have been detected in Sea King gearboxes [2] and vibration analysis has been involved on other occasions with Sea King aircraft in corroboration with the evidence obtained from oil and filter debris analyses, but no abnormal vibration has been detected in Wessex gearboxes. The same basic technique has been applied with great success to several other aircraft systems over more than a decade, enabling the detection of defective components before failure [3-6].

Why then did spectral analysis fail to detect the growing fatigue crack in the input bevel pinion in Wessex gearbox WAK143? This report shows that while spectral analysis is satisfactory for monitoring simple mechanical subsystems such as accessory gearboxes, there is an unexpected problem which limits its suitability for the detection of the subtle changes in vibration such as those which are caused by a fatigue crack in a gear in a complex system such as a helicopter gearbox. An alternative technique of vibration analysis called signal averaging is described which is better suited to the detection of local defects such as cracks in gears. It is demonstrated that signal averaging can give a clear indication of the existence of a crack in the input pinion in gearbox WAK143 more than 42 hours before failure. Also presented is a technique of digital signal processing for the enhancement of the effects of gear damage on the signal average which enables the presence of the crack to be detected more than 103 hours before failure. It is shown that the tooth meshing vibration in the signal average can be completely demodulated to reveal that the earliest indication of a crack in the gear is given by the appearance of a phase lag in the meshing vibration of the affected tooth. It is shown that for an advanced crack impacts excite resonances at low frequencies which offer a means of detecting advanced cracks. The material presented provides firm evidence that signal averaging and the associated enhancement

techniques offer a practical solution to the detection of cracks in the input spiral bevel pinion in the Wessex main rotor gearbox. These techniques are not restricted to the Wessex pinion but can be applied to other gears in the Wessex and to gears in other aircraft.

2. SPECTRAL ANALYSIS OF GEAR VIBRATION

2.1 Introduction

Any pair of simple involute gears in good condition produces vibration during operation due to the meshing action of the gear teeth. If the gears were perfect they would produce no torque variation and hence no vibration, but in practice the tooth profiles are always imperfect to some degree because of approximations in design, unavoidable errors in manufacture, deflection of the teeth, shaft and bearings under load, and wear of the tooth surface. The major part of the vibration is produced at the fundamental and harmonics of the tooth meshing frequency because the meshing vibration is not purely sinusoidal. The tooth meshing frequency is given by the number of teeth on the gear multiplied by the rotational speed and is the same for both gears in a simple pair. For the input spiral bevel pinion in the Wessex main rotor gearbox, which has 22 teeth and rotates at 42.7 Hz at nominal rotor speed, the tooth meshing frequency is approximately 940 Hz. In the amplitude spectrum of the vibration, the fundamental and harmonics of the gear tooth meshing frequency can usually be seen clearly. For example, Figure 5 shows the vibration spectrum from a jet engine accessory drive gearbox [6], indicating the fundamental tooth meshing frequencies of the two pairs of gears and several of their harmonics. The relative amplitudes of the fundamental and harmonics depend on the tooth profile errors but are also affected by the transfer function between the gear teeth and the vibration transducer which is usually mounted on the gearbox casing [7].

In addition to the components in the spectrum which are directly related to the meshing frequencies, there may be other components called modulation sidebands which appear about the meshing components separated from them by multiples of the shaft rotation frequency. Modulation sidebands are probably the most important indicators of the condition of a machine which can be found in the vibration spectrum. They are produced by the variations in the amplitude and phase of the tooth meshing vibration which repeat periodically with each revolution of the gear. The modulation of the meshing vibration in the time domain produces additional frequency components in the spectrum [8]. There will always be some low level modulation sidebands present in the spectrum because of the transmission errors present in the gears due to the unavoidable variations in the gear tooth spacing and profile. Eccentricity of a gear can produce large modulation sidebands as shown in Figure 6 due to the changes in amplitude of the tooth meshing vibration as the depth of mesh varies and the teeth move in and out of the correct mesh depth. Local defects such as tooth cracks should also produce modulation but the crack usually only affects the adjacent teeth when they mesh with the other gear and this only occurs for a short period each revolution of the cracked gear. The fact that the change is limited to a short period of each revolution has an important effect on the vibration spectrum, as the modulation sidebands which are produced extend over a very broad frequency range but at a very low amplitude, as illustrated in Figure 7. This has very important implications because in practice there is always a large background signal present from the operation of the gearbox due to the excitation of many minor structural resonances and the modulation components from other gears, all of which make it difficult to detect low level sidebands caused by a crack.

2.2 Weighting Functions

This situation is aggravated by a characteristic of spectral analysis performed using discrete data. In digital spectrum analyzers the spectrum is calculated from data which are sampled over a finite length of time. Implicit in this calculation is the assumption that the signal being sampled is exactly periodic within that time block [9], meaning that it repeats exactly and that no discontinuity exists between the samples at the beginning and end of this block and those occurring

before and after it. If these conditions are satisfied then the spectrum will be a true line spectrum. In practice the vibration signal is rarely periodic within the sampled block, producing a spectrum in which energy from each component may spread over many spectral lines as unwanted side lobes. Figure 8 shows an example of the amplitude spectrum, on a logarithmic scale, of a sinusoidal signal which is not periodic in the time block, illustrating clearly the additional spectral lines which are produced. The problem can be overcome by multiplying the time block by a weighting function or windowing function to force the beginning and end of the block to taper so that there is a smooth transition free of discontinuities between blocks. There are a great many weighting functions available with varying properties [10, 11]. Figure 9 shows the spectrum for the same sinusoidal signal after weighting by the commonly-used Hanning function [10, 11]. Note that there has been a drastic reduction in the level of the additional lines in the spectrum due to the effective removal of the discontinuities at the ends of the block. Figure 10 shows the spectrum for the same sinusoid after the application of an alternative weighting function known as a minimum four-term Blackman-Harris function [10, 11]. There has been a further reduction in the level of the side lobes but at the expense of a broadening of the main lobe which now covers about four discrete spectral lines. Obviously there must be a compromise between the level of the unwanted side lobes and the width of the main lobe, as reducing the levels of the side lobes increases the width of the main lobe. The type of weighting function selected can influence the ability to detect the modulation sidebands caused by local damage as the presence of large side lobes can make it difficult to detect low level sidebands while the broadening effect of the main lobe can cause closely spaced sidebands to merge into a continuous background.

2.3 Spectrum of WAK143

The spectrum of gearbox WAK143 at approximately 42 hours before failure as calculated by the Hewlett-Packard HP3582A spectrum analyzer at RAN Air Station at Nowra is shown in Figure 11. The spectrum was calculated from the last recording made before the crash on tape 29/83 at 1970.4 hours since new with a torque meter reading of 100 psi. The fundamental of the tooth meshing frequency of the input bevel pinion at 940 Hz and its second harmonic at approximately 1880 Hz are indicated. The second harmonic has a greater amplitude than the fundamental probably due in part to the form of the transfer function between the region of the tooth mesh and the location of the accelerometer on the gearbox casing [7]. One upper sideband can be discerned near the second harmonic.

One limitation of the HP3582A is its spectral resolution of only 256 lines which is aggravated by the provision of a 'flat top' weighting function [12] which has excellent low level side lobes and low picket fence losses but a very broad main lobe. Consequently the ability of the analyzer to separate closely spaced low level modulation sidebands without resorting to the zoom facility is limited. Figure 12 shows the spectrum obtained for the same recording calculated at ARL using a Spectral Dynamics SD335 analyzer which has a resolution of 500 lines and uses Hanning weighting. The greater resolution of the spectrum makes it possible to see that extensive modulation sidebands exist at an average spacing of about 43 Hz across part of the spectrum. Yet examination of the spectrum in Figure 13 obtained from another Wessex gearbox reveals similar modulation sidebands, although at slightly lower level, caused by the transmission errors in the gear. If modulation sidebands can be seen in the spectrum of a normal gear, how can a quantitative assessment of the condition of a gear be made?

One solution would be to reduce the many modulation sidebands present in the spectrum to a single peak which can be quantified by a single number. Cepstral analysis is a non-linear digital signal processing technique which was originally developed for the deconvolution of signals [13] but which can be used to search for patterns of modulation sidebands in a spectrum [14], producing a single line in the cepstrum at the frequency of the sideband spacing. But cepstral analysis is also affected by the weighting function, by additive noise, the presence of harmonics of the meshing frequency and by the resolution of the spectrum. A detailed analysis of its application to gear vibration is still being performed [15]. While the cepstrum may contribute in the future to the assessment of the spectrum there are many aspects of its use which are uncertain at present.

3. SIGNAL AVERAGING OF GEAR VIBRATION

3.1 Introduction

Originally almost all vibration analysis was performed in the time domain, simply because that was the only commonly available means. By the study of records such as Askania Vibrograph tapes it was possible to separate components of different frequency, albeit sometimes with difficulty. The development of spectrum analyzers, firstly the swept-sine analyzer, then the time-compression analyzer and finally the fast Fourier transform (FFT) analyzer, has made the study of the frequency spectrum of a vibration signal possible and made it easy to identify components at different frequencies in the spectrum. But a single gear pair can produce many frequencies, including the fundamental and harmonics of the tooth meshing frequency and modulation sidebands spaced at multiples of the rotation frequency of each of the gears. In a complex system some overlap of the components produced by each of the gear pairs must be expected and before the condition of the system can be assessed, the contributions of each gear pair must be separated. At present this is usually performed by a trained analyst who examines the spectrum. For simple gearboxes separation is relatively simple as there are only a few sets of meshing frequencies and harmonics [3-6], but for complex gearboxes with many gears and hence many more components, separation is correspondingly more difficult, particularly with the limited resolution provided by some analyzers.

Fortunately a technique called signal averaging offers an alternative to analysis in the frequency domain and provides the ability to separate the contributions of a single gear from the vibration of a complete gearbox, a task which in the vibration spectrum requires an analyst with considerable experience. The signal average produces a result in the time domain which may be presented as a graph of the vibration produced during one revolution of the gear of interest, including any variations in the pattern of the vibration during one revolution. Therefore the analyst can see whether modulation is occurring and should be able to recognize local defects such as fatigue cracks. There is no longer the need for extensive experience simply to separate the components, nor the need for a prior knowledge of the spectrum of a sound gearbox, as the signal average for a gear with a local defect contains the vibration from both the sound part of the gear and from the defective part. In principle, no other standard should be necessary, making it conceptually possible to decide the condition of the gear from a single observation.

3.2 Calculating the Signal Average

Figure 14 shows a schematic diagram of the equipment required for calculating the signal average of the vibration of a gear. A transducer such as an accelerometer is fitted to the gearbox case near the gear of interest, which in this example is marked *A*. The signal from the transducer is amplified and low pass filtered to remove high frequency components which are not required. A photoelectric or electromagnetic sensor fitted to the shaft on which gear *A* is mounted generates one electrical pulse during each revolution of the gear, so that the pulse train is locked in phase with the rotation of the gear. The signal averager itself may be a piece of purpose-built hardware or the operation may be performed by a small computer. On the first pulse after the start of averaging the instrument begins to sample the vibration signal, converting the analogue signal from the filter to a digital number which it stores in the averager memory. It continues to sample, convert and store throughout the remainder of the revolution. On the second pulse, the averager initiates sampling and conversion again, but this time stores the converted data in a separate block from the first. This process is repeated over many revolutions producing many blocks of data stored in the averager memory, with each block corresponding to the vibration produced by the gearbox during one revolution of the gear of interest. Then a process of ensemble averaging is performed. The value of the first sample in every block is added and divided by the total number of blocks to give the average value, which is stored as the first result in the output block. The process is repeated for the second sample in every block and the result stored in the second place in the output block. After repeating the process for all the samples in the block, the result is the signal average. If sufficient averages have been taken then all the vibration from the gearbox which is asynchronous with the rotation of the gear of interest will cancel out, leaving only the

vibration which is synchronous with that gear, namely the tooth meshing frequency and its harmonics and any modulation sidebands present.

Figure 15 illustrates the effect of signal averaging on a signal which is composed of a sine wave mixed with random noise having a peak-to-peak amplitude which is ten times that of the sine wave. In the original signal the sine wave cannot be discerned, but by performing signal averaging synchronized with the output of the oscillator which produced the sine wave, the latter can be extracted. The output of the white noise generator is not synchronous with the oscillator and so its effects can be reduced by averaging. After 100 averages the form of the sine wave can be recognized, and after 10 000 averages the sine wave is nearly free of noise. For the rejection of broad band noise in this manner, doubling the number of averages improves the signal to noise ratio of the signal average by a factor of $\sqrt{2}$ [16]. Fortunately the extraction of a signal from noise which consists primarily of discrete frequencies, as in a gearbox, can be achieved with a much smaller number of averages.

So far in this section signal averaging has only been considered qualitatively in the time domain but it can be shown that signal averaging is equivalent to a process of comb filtering in the frequency domain [16]. A comb filter has a series of pass bands of identical shape at a uniform frequency spacing so that the transfer function of the filter in the frequency domain resembles the teeth of a comb. When signal averaging is applied to the vibration of a gear, the teeth of the comb will be separated by the shaft rotation frequency. Signal averaging in the time domain is equivalent to multiplying the spectrum of the incoming signal by the comb spectrum thus passing only those frequencies which coincide with the comb teeth, namely the tooth meshing frequency and its harmonics together with all the modulation sidebands at the shaft rotation frequency. Increasing the number of averages taken reduces the width of the comb teeth and increases the depth between the teeth [16] thus making the comb filter more selective. Figure 16 shows the effect of increasing the number of averages on the shape of the teeth of the comb filter. After N averages the tooth half-width is $1/N$ of the tooth spacing.

3.3 Frequency Multiplication

In the above explanation it has been assumed that the gear rotated at an exactly constant speed and that sampling of the vibration signal occurred at a constant frequency, but in practice it is unlikely that the speed of a gear will remain exactly constant for more than a very short period of time. If the sampling frequency remains constant and the gear speed varies then the signal average, and particularly the later part, will become corrupted. Hence it is more usual to synchronize the sampling frequency itself with the frequency of the gear rotation so that if the machine speed increases or decreases then the sampling frequency will change also to compensate. One possible method of synchronizing the sampling and rotation frequencies is to generate many equispaced pulses per revolution of the gear using an electromagnetic or optical shaft encoder. However it is rarely convenient to generate more than a few pulses per revolution except under laboratory conditions. Instead an electronic instrument called a phase-locked frequency multiplier is used which accepts an input signal of one pulse per revolution of the gear and produces an output with the required number of pulses per revolution locked in phase with the input signal. Figure 17 shows a schematic diagram of the principal components of a digital phase-locked frequency multiplier. The signal from the input pulse train and the output of the divider having a ratio M enter a phase detector which determines the phase difference which exists between the leading edges of these signals and produces an error signal consisting of positive or negative pulses depending on the sign of the phase error and whose width is proportional to the magnitude of the phase error. The error signal is smoothed by a low pass filter to produce a steady voltage which drives a voltage-controlled oscillator (VCO). The frequency of the pulse train produced by the VCO is proportional to the input control voltage. The output of the VCO passes to the divider M and also to the divider D the output of which provides the output signal of the frequency multiplier. If the phase of the input signal advances slightly ahead of the output of the divider M then a positive error signal will be generated which will increase the output frequency of the VCO and advance the phase of the output to match the input. The output of the divider M thus follows the change in phase of the input signal. The reverse happens when the phase of the input signal retards slightly. In this manner the loop is

in principle able to track phase and frequency changes in the input signal. The ability in practice of the loop to capture and follow the input signal is determined by the gain of the phase detector, the characteristics of the low pass filter, the divider ratio M , the gain of the VCO and the rapidity of the changes in the input signal. Because the output of the VCO is divided by M before input to the phase detector, the loop will stabilize at a VCO frequency which is M times the input frequency, so that the output of the loop from the divider D is M/D times the input frequency.

It is common to process the signal average by computer, often involving calculation of the fast Fourier transform (FFT). The FFT is calculated most efficiently when the number of samples being transformed is an integer power of two, such as 64, 128, 256 or 512, therefore to reduce processing time it is common practice to select the number of samples per revolution of the gear to meet this criterion. For the input spiral bevel pinion which has 22 teeth, it is sufficient to resolve the tooth meshing vibration up to the fifth harmonic of the tooth meshing frequency, that is, at 110 cycles per revolution, or 110 shaft orders. Resolution of a signal at any frequency requires at least two samples per cycle, which in this case means 220 samples per revolution of the input pinion. Rounding up this number to the next largest power of two yields a minimum of 256 samples per revolution. In principle it should be possible to process the vibration of the input bevel pinion in the Wessex using a phase-locked frequency multiplier with $M = 256$ and $D = 1$, but in practice it is found that if the input signal contains some rapid frequency changes it is advisable to factorize a large value of M into several separate multipliers in series, each having a lower value of M .

Often it is not possible or convenient to obtain a pulse signal from the shaft on which the gear of interest is mounted, and this is the situation in the Wessex where the input shaft is not readily accessible. It is then necessary to take a pulse signal from another shaft in the system and to convert the frequency by appropriate selection of the values of M and D to obtain the sampling frequency required. In the Wessex aircraft the output of the alternator is available from power outlets in the cabin, and as the main rotor operates at a nominally constant speed no governor is fitted to the alternator, the output frequency of which is therefore directly proportional to the rotation frequency of the input pinion. During vibration monitoring flights, the alternator signal has been routinely recorded on channel 4 of the RAN Bruel and Kjaer 7003 recorder for several years to enable use of a Spectral Dynamics SD308-6 tracking adaptor with ARL's Spectral Dynamics SD335 spectrum analyzer. A four-stage phase-locked frequency multiplier has been designed and constructed specifically to take the alternator signal replayed from the tape recorder at 1.5 inches per second and produce a sampling signal at 256 pulses per revolution of the input bevel pinion in a form which is suitable for controlling the sampling of the vibration signal by a small computer [17]. This equipment forms the basis of a proposal for the routine application of signal averaging to the monitoring of the Wessex input bevel pinion [18].

Unfortunately there have been problems replaying some of the early tapes, including the four recordings made for gearbox WAK143 prior to failure, due to the excessive signal level of the alternator input to the tape recorder causing distortion of the recording which cannot be eliminated by filtering. This problem has since been overcome by the adjustment of the input attenuator on the RAN recorder and all subsequent tapes can be reproduced satisfactorily, but the analysis of the affected recordings has required special measures to be taken. It has been found that by band pass filtering the recorded vibration signal, not the alternator signal, in the range 1800 to 1900 Hz about the second harmonic of the input bevel pinion tooth meshing frequency using a Wavetek Rockland 751A filter which has a very sharp rolloff of 115 dB/octave, it is possible to obtain a clean signal with a frequency proportional to the rotation frequency of the gear. The spectrum of the signal after filtering is given in Figure 18 and it can be seen that the combination of the strong second harmonic and the sharp cutoff characteristic of the filter has been sufficient to depress the modulation sidebands about the meshing harmonic so that the largest sideband is approximately 18 dB below the peak. This is most important because the presence of significant sidebands here could have modulated the sampling signal and so produced spurious sidebands in the signal average. The filtered signal was passed to a Spectral Dynamics SD134A Tracking Ratio Tuner, which contains a single-stage phase-locked frequency multiplier enabling multiplication in the range 1 to 2000 and division in the range 1 to 9999. The filtered vibration signal was multiplied by 128 and divided by 11 to produce 512 samples per revolution of the input bevel pinion gear. Unfortunately it was not possible to use this tech-

nique on the vibration signal obtained from all of the Wessex gearboxes as its successful application required a large meshing vibration component with an amplitude well above that of the background signal. This was not always the case, but did enable the signal averaging of the recordings of WAK143 which would not have been possible otherwise due to the distortion of the recorded alternator signal.

3.4 Computer Implementation

The signal averaging of the Wessex recordings was performed by a Digital Equipment Corporation (DEC) PDP11 computer with a Datel Intersil Sinetrac LS12 analogue-to-digital converter board, running under the DEC RT-11 real-time operating system. All programs were written in the high-level language FORTRAN with the exception of the subroutines to perform the signal averaging which were written in the DEC assembly language MACRO to provide sufficient processing speed. Early versions of the programs were separated into two roles, firstly the calculation of the signal average, and secondly its subsequent analysis. The signal averaging program accepts digitized samples of the vibration signal produced by the analogue-to-digital converter at the leading edge of the pulses from the frequency multiplier and calculates the signal average for a specified number of samples per revolutions and number of averages. These calculations are performed using double-precision integer arithmetic to prevent arithmetic overflow during accumulation of the average. The resulting signal average is displayed on a computer terminal with a graphics capability and can be stored on a disc file for subsequent analysis.

3.5 Signal Average of WAK143

Figure 19 shows the signal average of the vibration of the input bevel pinion of gearbox WAK143 calculated using the computer and the band pass filtered vibration signal with the Spectral Dynamics SDJ34A frequency multiplier as described. It was derived from the last RAN recording on tape 29 83, made about two months prior to failure, at 1970.4 hours since new, or approximately 42 hours before failure. The torque meter pressure was 300 psi and 256 averages were taken. The signal average shows at first the normal pattern of vibration at the second harmonic of the tooth meshing frequency, giving 44 cycles per revolution. Near the centre of the trace there is a transient as the cracked part of the gear meshes with the crownwheel, after which the perturbation decays slowly and the trace returns to the normal meshing pattern. For comparison Figure 20 shows the signal average for the input bevel pinion in another Wessex gearbox, in which there is some modulation of the meshing vibration but no sharp transients are present. Therefore it is clear that a simple visual inspection of the signal average at 42 hours before failure can give a positive indication of the abnormal meshing behaviour which is occurring. From Figure 3 it can be estimated that the crack may have been more than 25 mm long and 3 mm deep at this time.

Figure 21 shows the signal average of the input pinion in gearbox WAK143 made from the second last RAN recording on tape 14 83, at 1909.5 hours since new or approximately 103 hours or five months before failure. The torque meter pressure was 440 psi and 256 averages were taken. The normal pattern of vibration appears at the second harmonic of the tooth meshing frequency with some slow modulation present, but there is no transient and no indication of abnormal meshing as was seen in Figure 19. This signal average is virtually indistinguishable from the signal average of the sound gear seen in Figure 20 yet it can be estimated from Figure 3 that the crack may have measured approximately 20 mm long by 1.2 mm deep at the time of this recording. It would therefore seem that the crack cannot be detected by simple visual inspection of the signal average at 103 hours before failure, and that the earliest warning which might be expected would be between 103 and 42 hours before failure. Certainly this warning is useful, but if 25 operating hours is taken as the typical interval between vibration recordings which are made in service, there may be only one or at most two chances to detect the crack. Earlier warning of the presence of the crack would seem highly desirable.

4. ENHANCEMENT OF THE SIGNAL AVERAGE

4.1 Introduction

It is interesting to consider why there should be no visible evidence of the crack in the signal average produced from the recording of gearbox WAK143 at 103 hours before failure when the crack may have measured 20 mm by 1.2 mm at this time. The answer becomes clear when the amplitude spectrum of the signal average, shown in Figure 22, is examined. Because the signal average is exactly periodic in the time domain the spectrum is a pure line spectrum, free of the problems of weighting functions and side lobes discussed previously. The horizontal axis of the spectrum is graduated in multiples of the shaft rotation frequency, known as shaft orders, so that the fundamental of the tooth meshing frequency appears at 22 shaft orders, although it has only a small amplitude. At 25 shaft orders there is a larger component which is not related to the tooth meshing but at present is believed to be what is called a ghost component caused by transmission errors in the gear originating from errors in the machines used for gear manufacture. Ghost components are not common but are occasionally reported [14]. The largest component in the spectrum is the second harmonic of the tooth meshing frequency at 44 shaft orders with an amplitude of 6.4 g, approximately seven times the amplitude of the next largest component. About the second harmonic there exists a cluster of modulation sidebands which extend from approximately 30 shaft orders to 58 shaft orders. Modulation sidebands are also present about the other meshing harmonics but at a lower level. Note that all the modulation sidebands are very small, and that the component at 44 shaft orders has an amplitude about 10 times that of the largest sideband, which is smaller even than the ghost component. It is the low level of the modulation sidebands relative to the major spectral components which explains why there is no visible evidence of the crack in the signal average. The modulation is only very slight compared to the amplitude of the second harmonic of the tooth meshing frequency. To enable the crack to be detected in this signal average requires enhancement of the average by some technique of digital signal processing in order to extract the relevant information. Several techniques have already been developed [19] and one of these will now be described.

4.2 Elimination

An enhancement technique known as FM4 [19] eliminates the major known components from the spectrum, including the fundamental of the tooth meshing frequency and its harmonics and possibly some of the modulation sidebands if necessary. For example, in the case of the Wessex input bevel pinion, the meshing harmonics at 22, 44, 66 shaft orders and so on could be eliminated and possibly the modulation sidebands at 21, 23, 43, 45, 65, 67 shaft orders and so on. For the elimination process to be successful, the user requires some experience of which components are normally present in the spectrum and which components are more likely to represent an abnormality, and these findings are likely to be different for each different gearbox and gear type. After elimination of the components from the spectrum, the corresponding time domain signal is calculated. Since the major meshing components have been eliminated it might be expected that the remaining components describe the departures of the vibration from the normal pattern of vibration.

The effect of elimination can be explored by eliminating the components at 22, 44, 66, 88 shaft orders and so on from the signal average for 103 hours before failure. The resulting time domain signal is shown in Figure 23. While there are still many apparently random fluctuations present it is now possible to see a large oscillation near the centre of the trace which is believed to be caused by the crack in the gear. This is a clear indication that enhancement of the signal average can improve the ability to detect local gear defects.

4.3 Kurtosis

As discussed in an earlier section, one of the many problems with spectral analysis is that the many modulation sidebands which may be produced by a local defect in a gear are difficult to assess quantitatively so as to provide some measurable result of the analysis. A similar problem can exist with the assessment of the enhanced signal average, but fortunately the solution is

much simpler because it can be assumed that a defect, if present, will usually be restricted to a small part of the gear. Hence in the signal average the abnormal vibration will be restricted to a small part on the revolution. Any technique for assessing the signal average should therefore seek to quantify the damage by detecting any isolated peaks which may appear in the enhanced signal average. Several parameters have been proposed for this purpose [19] including the crest factor, which is the ratio of the peak-to-peak value of a signal to its root-mean square value. The crest factor is typically 2.8 for a sine wave and any increase in the peakiness of a signal will increase the crest factor above this value. One shortcoming of the crest factor as a means of assessing the enhanced signal average is its incorporation of the peak-to-peak value, as the presence of a single very narrow peak will produce the same peak-to-peak value as a broader peak of the same size. The root-mean-square value for the signal with the broader peak will be larger than that for the narrow peak and hence the crest factor will be less for the broader peak than for the narrow peak.

This can be overcome to some extent by the use of an alternative parameter which is the normalized fourth statistical moment, commonly known as the kurtosis [20]. For a population X the kurtosis K is given by the following equation:

$$K = \frac{\sum (X_i - M)^4}{N S^4} \quad (1)$$

where

N = number of samples

M = mean value

S = standard deviation

A normal or Gaussian distribution has a kurtosis of 3.0 while for a sine wave the kurtosis is 1.5. The presence of any large isolated peaks in the signal produces larger tails in the distribution of the samples and consequently increases the kurtosis. This principle has already been used successfully for the analysis of the vibration produced by rolling element bearings with spalling damage [21] and has also been applied to the assessment of enhanced signal averages of gear vibration [19]. Because the numerator of Equation 1 is derived from all of the values in the population, unlike the peak-to-peak value in the crest factor, it does respond to multiple peaks. Very broad peaks will increase the value of the denominator and bring about a reduction in the kurtosis, but it does appear to be less sensitive to this problem than does the crest factor.

4.4 Application

For the original signal average shown in Figure 21 the kurtosis is calculated to be 1.7, falling in between the values of 1.5 for a sinusoid and 3.0 for a random signal. After enhancement of the signal by removal of the meshing-related components as shown in Figure 23, the kurtosis is 4.6. Hence the simple process of eliminating the meshing-related harmonics increases the kurtosis noticeably. Recordings of the vibration of other Wessex gearboxes have been analyzed in this manner. Most of the kurtosis values fall within the range 2.5 and 3.5. While the kurtosis for WAK 143 at 103 hours before failure is outside the range presented for the other gears, the change in kurtosis represents only a small departure, suggesting that the enhancement procedure is not sufficiently powerful to make a clear distinction. A better enhancement procedure would be desirable.

4.5 Ghost Component

It will be recalled that Figure 22 showed a large spectral component at 25 shaft orders which is believed to be a ghost component resulting from errors in the manufacturing process. The elimination of the meshing related components does not of course remove this ghost and yet its amplitude is greater than the biggest of the modulation sidebands. If the ghost component is eliminated as well as the meshing components then the information contained in the modu-

lation sidebands may be more apparent. The resulting enhanced signal average at 103 hours before failure is shown in Figure 24. There is a noticeable improvement in the clarity of the signal and an increase in the kurtosis from 4.6 to 6.6. This suggests that it may be important to eliminate not only the meshing related components but also other large components which may not be related to the modulation sidebands.

4.6 Conclusions

It has been shown that the application of some simple digital signal processing techniques to the signal average can enhance the information produced by the local damage and can reveal the presence of the crack which could not otherwise be detected. It has also been shown that the enhanced signal average can be assessed using the kurtosis of the signal, as disturbances in the enhanced signal average such as those caused by the crack can cause an increase in the kurtosis. It was observed that the application of the same procedure to the signal averages of normal gears revealed considerable scatter in the kurtosis. The difference in the kurtosis between the cracked gear and the normal gears was not sufficient for a confident diagnosis of early cracks. So far the arguments proposed to explain the principle of the enhancement procedure are only qualitative and no theoretical basis for it has been proposed. There has been no explanation of what exactly the enhanced signal average represents and at present it cannot be interpreted in terms of the modulation which is caused by the crack in the gear.

5. NEW TECHNIQUE FOR ENHANCEMENT

5.1 Introduction

In the previous section it was shown that an existing enhancement technique can reveal the existence of the crack in the input bevel pinion of gearbox WAK143 when it was not visible in the original signal average. Unfortunately this technique, developed empirically, has no firm theoretical basis. In this section an alternative new enhancement technique [22] will be developed which permits the interpretation of the enhanced signal in terms of the modulation produced by the crack in the gear.

5.2 Development

Consider two gears which mesh under a constant load at constant speed, and assume initially that all the teeth on the gears are identical and are equally spaced. The meshing vibration $x(t)$ of one of the gears may be represented by the fundamental and harmonics of the tooth meshing frequency f_N

$$x(t) = \sum_{m=0}^M X_m \cos(2\pi m f_N t + \phi_m) \quad (2)$$

Now assume that the gear has a local defect which will produce short term changes in the amplitude and phase of the meshing vibration as the defect goes through the mesh. These changes are described by the amplitude and phase modulation functions $a_m(t)$ and $b_m(t)$ respectively, and as these functions are periodic with the gear rotation frequency f_r , they can be represented by finite Fourier series

$$a_m(t) = \sum_{n=0}^N A_{mn} \cos(2\pi n f_r t + \alpha_m) \quad (3)$$

$$b_m(t) = \sum_{n=0}^N B_{mn} \cos(2\pi n f_s t + \beta_m) \quad (4)$$

The modulated gear meshing vibration $y(t)$ is given by:

$$y(t) = \sum_{m=0}^M X_m (1 + a_m(t)) \cos(2\pi m f_x t + \phi_m + b_m(t)) \quad (5)$$

In the frequency domain, the Fourier transform of the above function will comprise the fundamental and harmonics of the meshing frequency surrounded by modulation sidebands, and unless the number of teeth $T > 2N$ there will be interference between the high-order sidebands of adjacent meshing harmonics. The extent of this interference will depend on the form of the modulation, which determines the strength of the high-order sidebands, and also on the relative amplitudes of the meshing harmonics. A strong meshing harmonic of amplitude X_m will produce corresponding strong sidebands.

If the signal average is band pass filtered about one of the meshing harmonics m with a bandwidth W , then provided the amplitude of that harmonic is much greater than its neighbours, the interference from the sidebands of the neighbouring harmonics will be small. If the filter bandwidth is chosen so that $W < 2(T - N)f_s$ then the sidebands from neighbouring meshing harmonics will be completely excluded from the pass band. However if the bandwidth $W < 2Nf_s$ then some of the high order sidebands of the selected harmonic will be excluded from the pass band. On the other hand, selecting $W = 2Nf_s$ will pass all of the desired sidebands, and some of the interfering sidebands as well. However, if it is assumed that the amplitude of the selected meshing harmonic is much greater than the amplitude of the neighbouring harmonics, then the interference will be small, and the filtered signal can be approximated by:

$$z_m(t) \approx X_m (1 + a_m(t)) \cos(2\pi m f_x t + \phi_m + b_m(t)) \quad (6)$$

This function describes the vibration which is produced at the contact area of the gear teeth. Unfortunately, direct measurement of this vibration is rarely practicable, and it is usual to measure the gear vibration with a transducer mounted on the exterior of the gearbox case. The vibration from the contact area must therefore pass through the gears, shafts, bearings and case before reaching the transducer. Consequently the broad band vibration may be modified considerably by the transfer function between the gear teeth and the transducer, and there is no simple technique for removing these effects. It will be assumed here that the changes in the transfer function across the bandwidth W of the band pass filter are small and can be neglected. It is shown in the Appendix that provided $|b_m(t)| \ll \pi$ and $|a_m(t) \cdot b_m(t)| \ll 1$, then $z_m(t)$ can be approximated by:

$$z_m(t) \approx X_m [\cos(2\pi m f_x t + \phi_m) + a_m(t) \cos(2\pi m f_x t + \phi_m) - b_m(t) \sin(2\pi m f_x t + \phi_m)] \quad (7)$$

The filtered residual $r_m(t)$ is obtained by subtracting the meshing component at frequency $m f_x$ from the band pass filtered vibration:

$$\begin{aligned} r_m(t) &= z_m(t) - X_m \cos(2\pi m f_x t + \phi_m) \\ &\approx X_m [a_m(t) \cos(2\pi m f_x t + \phi_m) - b_m(t) \sin(2\pi m f_x t + \phi_m)] \\ &= X_m \sqrt{a_m^2(t) + b_m^2(t)} \\ &\quad \cos(2\pi m f_x t + \phi_m - \tan^{-1}(b_m(t)/a_m(t))) \end{aligned} \quad (8)$$

Note that the filtered residual still contains vibration at the frequency mf_x which was passed by the band pass filter, even though the meshing harmonic itself has been eliminated. To remove this vibration, the envelope $e_n(t)$ of the filtered residual can be calculated:

$$e_n(t) \approx X_m \sqrt{a_m^2(t) + b_m^2(t)} \quad (9)$$

Hence by band pass filtering the signal average, eliminating the dominant meshing harmonic and enveloping, a function is obtained which is directly related to both the amplitude and phase modulation.

5.3 Application

Figure 22 shows the spectrum of the signal average for gearbox WAK143 at 103 hours before failure. The largest component occurs at 44 shaft orders, the second harmonic of the tooth meshing frequency, and about this component there occurs a large cluster of modulation sidebands which decrease in amplitude with increasing separation from the central peak. On the low frequency side of the second harmonic the sidebands reach a minimum at about 30 shaft orders, presumably where the sidebands from the fundamental meshing component and the second harmonic meet. There is a corresponding point on the high frequency side of the second harmonic at about 58 shaft orders. Both of these minima are 14 shaft orders above and below the second harmonic at 44 shaft orders. In terms of Equations 3 and 4, $m = 2$ and $N = 14$. The signal average can be band pass filtered by setting the amplitudes of all the spectral lines which lie outside the range 30 to 58 shaft orders inclusive to zero and calculating the corresponding time domain signal from the modified spectrum, giving the result shown in Figure 25. The filtered signal average has a much cleaner appearance than the original signal average in Figure 21 because the high and low frequencies outside the pass band have been removed. There is some slow modulation of the signal but no transients. The kurtosis of the filtered signal is 1.6, which is close to the value of 1.5 expected for a sine wave because the filtered signal is dominated by the meshing harmonic at 44 shaft orders.

The second step in the enhancement process is to eliminate the meshing harmonic by setting the amplitude of the component in the spectrum at 44 shaft orders to zero and calculating the corresponding time domain signal from the modified spectrum to give the result shown in Figure 26. There can now be seen a large oscillation near the centre of the trace which is similar to that seen in Figures 23 and 24. The kurtosis of this signal is 7.0 with the increase being caused by the oscillation. Note that the frequency of the oscillation is 44 shaft orders, even though the component at 44 shaft orders was eliminated from the spectrum. This is an example of modulation with complete suppression of the carrier. The oscillation does not provide any additional information and it is only the envelope of the signal that is of interest. The envelope can be calculated using the Hilbert transform of the signal [23] as follows. Firstly calculate the forward Fourier transform of the signal and then set the amplitude of all the spectral components at negative frequencies to zero and double the amplitudes of the spectral components at frequencies above zero while leaving the component at zero frequency unchanged. In this way a complex spectrum has been created from the original real spectrum. Then calculate the inverse Fourier transform of the complex spectrum, giving a result which is a complex time domain signal called the analytic signal [23] which can be viewed as a rotating vector as shown in Figure 27. The real signal which is observed in practice can be considered as the projection of the analytic signal onto the plane formed by the real and time axes. The imaginary part is the projection onto the plane formed by the imaginary and time axes. The envelope of the real signal is given by the amplitude of the rotating vector which can readily be obtained from the real and imaginary signals using Pythagoras' theorem. All of the above procedures can be readily implemented on a small digital computer using the fast Fourier transform.

The envelope calculated from Figure 26 is shown in Figure 28. The original oscillation seen in Figure 26 has been replaced by a large peak near the centre of the trace providing clear evidence of the existence of the crack in the gear at this time. The kurtosis of the enveloped signal is 9.2, a very large increase over the kurtosis which was obtained previously. Note also

the presence of the other low level peaks which occur elsewhere in the enhanced signal. There are several possible sources for these peaks, the first being that they are caused by genuine amplitude and phase modulation produced by transmission errors in the gear, and as these errors are essentially random the background peaks have a random appearance. The second possibility is that they are systematic errors caused by the approximations in the analysis, including the truncation of the high-order sidebands which fall outside the pass band of 30 to 58 shaft orders and also the admission of high-order sidebands of other harmonics of the meshing frequency. They also may be caused by the additional non-linear terms present because the modulation may not be small and consequently the approximations in Equation 7 may not be strictly valid.

Band pass filtering of the signal average can restrict the resolution of features in the enhanced signal due to the limited number of frequency components which are passed. In this instance the filter has a half-width of 14 shaft orders, while the input bevel pinion has 22 teeth and a contact ratio which is greater than 1.5. Any reduction in the stiffness of one tooth due to a crack will affect the meshing of the adjacent teeth as some of the load which cannot be borne by the cracked tooth is transferred. The affected region may extend to the width of the contact region and thus exceed $1.5 \times 1/22$ or approximately 1.14 revolutions wide. Therefore it would seem reasonable that a filter half-width of 14 shaft orders should be more than adequate to resolve the affected region.

Note that the amplitude of the peak in the enhanced signal average may not be important. The amplitude is directly proportional to the amplitude of the meshing harmonic X_m as shown in Equation 9, but so will be the amplitude of other peaks in the enhanced signal. More important than the absolute amplitude is the detection of any isolated peaks which appear above the remainder of the enhanced signal and it would appear that the kurtosis may be able to do this.

5.4 Other Gearboxes

Although the spectrum of gearbox WAK143 was dominated by the second harmonic of the tooth meshing frequency this is not so for all other gearboxes. Most have a dominant fundamental tooth meshing frequency in which case separation can be performed by band pass filtering in the range 8 to 36 shaft orders and eliminating the component at 22 shaft orders, thus maintaining the half-width of the filter the same at 14 shaft orders. If any other harmonic of the meshing frequency was dominant the appropriate procedure could be applied. Recordings of the vibration of other Wessex gearboxes have been analyzed in this manner, and most kurtosis values fall within the range 1.9 to 3.3, with the majority of the values lying between 2.0 and 3.0. In isolated instances values as high as 4.5 have been obtained repeatedly from normal gears but these are considered to be exceptional. The majority of the values for normal gears are far removed from the value of 9.2 achieved earlier for the cracked gear. The effectiveness of the new technique of enhancement compared with the traditional enhancement technique can be seen in the greater change in the kurtosis achieved for the same signal average.

6. DEMODULATION OF THE SIGNAL AVERAGE

6.1 Introduction

In the previous section a new enhancement technique for signal averages was described in which the result obtained incorporated both amplitude and phase modulation terms. Several approximations made in the analysis limited the direct applicability of the theory to small values of modulation. In this section the analysis will be extended to show that the signal average of the gear vibration can be completely demodulated enabling the separation of the amplitude and phase modulation terms [24]. This new technique is not restricted to small modulation, and demonstrates the great importance of phase modulation.

6.2 Development

As described in Section 5.2, the signal average of the vibration generated by a gear after band pass filtering about one of the major meshing harmonics is given by:

$$z_m(t) \simeq X_m(1 + a_m(t)) \cos(2\pi m T f_s t + \phi_m + b_m(t)) \quad (10)$$

The equation for $z_m(t)$, which was expressed as a cosine function, can be viewed as the real part of a complex function $c_m(t)$ known as the analytic signal and defined by:

$$c_m(t) = z_m(t) - jH(z_m(t)) \quad (11)$$

where $H(z_m(t))$ is the Hilbert transform of $z_m(t)$ [23]. In Figure 27, the analytic function is shown as a rotating vector with the real part $z_m(t)$ being the projection of the vector on the real plane defined by the time axis and the real axis. As time progresses, the vector rotates about the time axis with an average rotation frequency of mTf_s . By substituting Equation 10 into Equation 11, it can be shown that:

$$c_m(t) = X_m(1 + a_m(t)) e^{j(2\pi m T f_s t + \phi_m + b_m(t))} \quad (12)$$

It is clear from the above that the length of the vector is subject to variations $X_m a_m(t)$ due to the amplitude modulation, while the uniform rotation of the vector is disturbed by phase variations $b_m(t)$ due to the phase modulation. Estimates of the modulation functions $a_m(t)$ and $b_m(t)$, subject to the assumptions and approximations in deriving Equation 10, can be readily obtained by:

$$a_m(t) = |c_m(t)| / X_m - 1 \quad (13)$$

$$b_m(t) = \arg(c_m(t)) - (2\pi m T f_s t + \phi_m) \quad (14)$$

6.3 Application

The new demodulation technique is demonstrated by applying it to the signal average obtained from the recording made at 103 hours before failure which was shown in Figure 21. The filter pass band is set to cover the range 30 to 58 shaft orders inclusive, as for the enhancement technique already described. Firstly the amplitudes of all spectral components outside the range 30 to 58 shaft orders are set to zero. Secondly, the amplitudes of all spectral components at negative frequencies are set to zero and the spectrum is translated to locate the component which was at 44 shaft orders to 0 shaft orders. The original real spectrum has now been converted to a complex spectrum because it is no longer symmetrical about zero frequency. The complex spectrum is then converted to the time domain by the inverse Fourier transform to give a complex signal which describes the analytic vector, except that translation has removed the uniform rotation of the vector and so the vector remains approximately stationary. Amplitude modulation of the meshing vibration causes the length of the vector to vary while phase modulation causes the vector to rock back and forth. The amplitude and phase of the vector can be calculated from the real and imaginary components.

Figure 29 shows the amplitude of the vector calculated from the signal average at 103 hours before failure. It shows that small random variations occur in the amplitude but there is no marked change at the location of the defect. This is to be expected since no strong amplitude modulation was seen in the original signal average. The phase of the vector is shown in Figure 30. Small random variations are also seen but there is also a marked phase lag of approximately 60 degrees at the location of the defect. This is an extremely interesting result as it suggests that the very early indications of a crack may be first given by the phase modulation. The crack reduces the stiffness of the affected teeth causing deflection of the teeth under load, delaying the generation of the vibration by those teeth and so producing a phase lag. A lag of approximately

60 degrees at 44 shaft orders corresponds to a delay of approximately 1.5 degrees at the shaft rotation frequency. The phase modulation cannot be readily discerned in the original signal average without prior knowledge. Assessment of the original signal average is usually based on the detection of amplitude modulation by such parameters as the crest factor and the kurtosis which are ill suited to the detection of phase modulation. Only enhancement by the old [19] or new [22] methods makes possible the detection of the phase modulation.

Demodulation can also be applied to the signal average obtained for the recording made at 42 hours before failure which was shown in Figure 19. Using the same analysis technique, the amplitude of the vector is shown in Figure 31, and it can be seen that the amplitude falls to nearly zero at two locations. The phase of the vector is shown in Figure 32, indicating that there is a complete reversal of phase at one location representing a loss of 360 degrees. In this instance the separate amplitude and phase diagrams are difficult to interpret, but they can be combined into a single polar diagram with the tail of the vector fixed at the origin. As time passes the head of the vector traces out a locus which is shown in Figure 33 for the recording at 103 hours before failure and in Figure 34 for the recording at 42 hours before failure. Both traces have been oriented so that the average phase is set to zero thus lying along the real axis. A decrease in phase causes the vector to rotate clockwise about the origin. For a gear in undamaged condition it would be expected that the locus would be confined to a compact bundle about the real axis because the amplitude and phase modulation would be small. For the early crack in Figure 33 the locus departs clockwise from the bundle and rotates approximately 60 degrees indicating a phase lag with little variation of amplitude, while for the advanced crack in Figure 34 the locus again departs clockwise but does not return as soon as for the early crack. Instead, the locus completely encircles the origin in a clockwise direction, with the amplitude falling close to zero as the phase reversal occurs and then increasing. This produces the first dip in the amplitude signal shown in Figure 31. The phase reversal in Figure 32 occurs when the locus crosses the negative real axis. After the first loop about the origin, the locus nearly completes a second loop with the amplitude again falling nearly to zero before returning to the bundle. The complete loop indicates the complete loss of 360 degrees of meshing vibration, which can be interpreted as the loss of one cycle of the second harmonic of the meshing frequency. The completion of the second loop about the origin, had it occurred, could have been interpreted as two cycles of the second harmonic missing, and could have implied that one tooth on the gear was carrying no load at all.

7. EXCITATION OF RESONANCES BY GEAR TOOTH IMPACTS

7.1 Introduction

All of the techniques considered so far have concentrated on the analysis of the vibration at the tooth meshing frequency and its harmonics, searching for modulation of the meshing vibration. In addition to the modulation of the tooth meshing, it is known that local defects in gears such as surface pits and fatigue cracks can also produce impulses or impacts with energy over a wide frequency range [14, 25, 26]. This section reviews the characteristics of such impacts and then examines the use of the signal average for the isolation of the low frequency vibration generated by gear tooth impacts and its application to gearbox diagnostics.

7.2 Development

A simple model has been proposed [14] in which the vibration produced by gear defects is expressed in terms of the amplitude and frequency modulation of the normal gear meshing vibration plus additive impacts, and it has been suggested that most local defects will generate both of these effects. In the frequency domain, the components produced by the impacts may be observed at low frequencies and/or across the spectrum. Spalling damage of gear teeth has also been detected from the impacts produced [25]. The signal average of the gear vibration is the superposition of the tooth meshing vibration and the resonances excited by the impacts, and

as some resonances may occur at comparable frequencies to the meshing frequency and harmonics, adaptive signal processing techniques may be necessary to detect the resonances. Very high frequencies, in excess of 25 kHz, have been detected from gears with fatigue cracks [26]. By band pass filtering and demodulating this vibration, a pulse train is produced with a frequency corresponding to the frequency with which the impacts occur. From these examples it is clear that the frequencies excited by gear tooth impacts can extend from low to very high, probably because the resonances excited by the impacts come from many different sources, including the gears, shaft and bearings, the machine case, the vibration transducer and the signal conditioning equipment such as amplifier and filter.

The very high frequencies used for impact detection [26] are well above the normal gear tooth meshing frequencies and so can be isolated very simply by a band pass filter. However if the original vibration signal is to be recorded for off-line analysis, the very high frequencies present will require a recorder with a large bandwidth. At the low frequencies sometimes used [25] recorder bandwidth is unlikely to be a problem, but separation of the resonances from the gear meshing vibration is more difficult. Nevertheless, the signal averaging approach has proved to be very successful in the identification of gear defects. One factor in its favour is that the signal average is exactly periodic in the time domain, permitting simple conversions between the time and frequency domains without the need for weighting functions, thereby making possible the filtering of the signal in the frequency domain. While the adaptive technique is successful, a simpler alternative would be attractive. Given that impacts may be observed at low frequencies [14], it should be possible to examine the signal average of the vibration of a gear for signs of a resonance below the tooth meshing frequency, and in favourable circumstances, it may be possible to isolate the resonance from the gear meshing and modulation sidebands by low pass filtering the signal average in the frequency domain.

At this stage it is worth considering why impacts should occur. It has already been shown that an early fatigue crack in a gear tooth will allow deflection of the tooth under load, resulting in a phase lag in the meshing vibration of that tooth. While no formal model for the production of impacts has been proposed, it is presumed that an early fatigue crack only affects the stiffness of a small sector of the gear, and that provided the sector is sufficiently small, there will always be another sound tooth in contact to carry the load. For this to be true the affected region must be less than the contact ratio minus one. As the crack grows, the size of the affected region will increase until it is greater than the contact ratio minus one, so that for a period of the tooth engagement only the unsound tooth will be in contact. The exact behaviour then is uncertain, but it may be that the greater deflection of the affected region will be sufficient to cause relative misalignment of the following teeth on the two gears so that an impact is produced when these teeth meet and resume their correct relative positions. Alternatively, it may be that as the preceding sound tooth ceases contact the affected tooth will be unable to maintain the same load because of its reduced stiffness. The sudden reduction in the tooth contact force will be transmitted as an impact through the gear to the bearings and then through the casing.

The detection of low frequency gear impacts independent of the tooth meshing vibration could be a useful contribution to machinery diagnostics by providing an indicator of the severity of the damage to a gear [27]. If impact generation is determined by the size of the affected region relative to the contact ratio, then the presence of impacts implies that a crack is no longer small but has grown to the stage where the load can no longer be borne by the adjacent tooth. The larger forces associated with the impacts can be expected to accelerate the deterioration of the gear.

7.3 Application

Figures 35 and 36 show the low frequency part of the vibration spectra produced from the signal averages at 103 and 42 hours before failure respectively. At 103 hours there are only low amplitudes at multiples of the shaft speed, while at 42 hours before failure the spectrum has changed considerably with the appearance of components of significant amplitude. Note in particular the growth of the low frequency components in the range below 18 shaft orders. These are unlikely to be modulation sidebands from the fundamental meshing component at

22 shaft orders because the amplitude of this component is too small, and they are very unlikely to be lower sidebands of the second harmonic at 44 shaft orders because they are so far removed. Presumably these components are a low frequency resonance excited by the impacts.

To isolate the presumed resonance from the tooth meshing components, sidebands and ghost component, both signal averages were filtered to pass components in the range 0 to 18 shaft orders inclusive, giving the signals shown in Figures 37 and 38. Filtering was performed in the frequency domain by setting the amplitudes of the spectral lines outside the pass band to zero. The phase spectrum was not modified. On transforming back to the time domain, the filtered signal was produced. Figure 37 shows only small random departures from the origin, but Figure 38 shows a strong transient decaying oscillation consistent with a decaying resonance with its leading edge located approximately at the location of the crack. Measurement of the frequency of oscillation shows it to be close to 15 cycles per revolution, corresponding to the largest spectral peak in the pass band.

While the transient oscillation is clear to the observer, it would be valuable to have a parameter which could be used to assess the condition of the filtered signal to assist with computer-aided machinery monitoring. In earlier sections, the kurtosis has been used to assess enhanced vibration data with success. For Figure 37 the kurtosis of the filtered signal is found to be 3.5, while for Figure 38 the kurtosis is 6.9.

7.4 Discussion

The oscillation at approximately 15 cycles per revolution seen in the filtered signal average in Figure 38 for the large crack was not visible in the signal average of Figure 19. This is probably because several resonances are present in the signal, but are difficult to recognize in the spectrum of Figure 36 against the strong meshing components and modulation sidebands. The summation of all the resonances present would give a very different waveform from that in Figure 38, with a better defined leading edge. If the transfer function or frequency response of the system between the gear tooth contact and the vibration transducer was uniform and complete elimination of the meshing components and their modulation sidebands was possible, then the shape of the observed impact would approach that of an ideal impulse. It is the resonances in the transmission path, apparent as local peaks in the transfer function, which produce the oscillation when excited by an impulse, demonstrating the importance of the transfer function on the successful detection of low frequency impacts. It has been shown [7] that the location of the transducer can affect the measured tooth meshing component and modulation sidebands, and similarly poor transmission of the vibration at frequencies below the fundamental tooth meshing frequency could impair the detection of impacts.

Machine mounting conditions may also affect the low frequency transmission characteristics. The data presented here were obtained from a gearbox mounted in an aircraft. The spectra of signal averages obtained for another cracked gear of the same type in a gearbox mounted in a test bed instead of an aircraft [28] showed that most of the components at frequencies below the third harmonic of the meshing frequency were suppressed, probably due to the stiffer mounting of the gearbox. Low pass filtering of these signal averages in the range 0 to 18 shaft orders did not produce a transient oscillation, hence it would appear that a strong low frequency resonance is necessary for the proposed technique to work.

Another major factor to consider is the strength of the tooth meshing vibration. In the example presented here the fundamental meshing component at 22 shaft orders is very small, and consequently the modulation sidebands about it are small. This permits the low pass filtering up to 18 shaft orders, close to the fundamental meshing component, yet still giving good separation of the resonance. The meshing component itself can be readily eliminated from the spectrum, but had the meshing component been larger, then any sidebands present about it would have intruded into the range below 18 shaft orders and prevented proper isolation of the resonance. In practice, it is likely this intrusion will occur. Fortunately many resonances may be excited at higher frequencies, even above the higher harmonics of the meshing frequency. Previously spectrum analysis has been used to examine the pulse produced by isolating and demodulating these high frequency resonances [26], but signal averaging of the modulated resonances could also be used. It is hoped that this aspect can be investigated in a future work.

7.5 Conclusions

The vibration produced by gears with local defects such as advanced fatigue cracks may include resonances at low frequencies which are excited by impacts between the gear teeth. In favourable circumstances it is possible to isolate one or more of these resonances from the tooth meshing vibration and modulation sidebands by low pass filtering the vibration signal so that the filtered signal displays a damped oscillation which commences at the location of the fatigue crack. The successful application of the technique depends on the form of the transfer function between the gear teeth and the transducer, and on the strength of the fundamental tooth meshing component. The existence of a strong resonance at a low frequency will assist in the detection of impacts, while the absence of a strong component at the fundamental tooth meshing frequency will enable better isolation of the resonance from the meshing component and its sidebands. While both of the above conditions exist in the recordings of gearbox WAK143, there will be many instances in practice where conditions are less favourable.

8. CONCLUSIONS

Following the crash of an RAN Wessex helicopter caused by the catastrophic fatigue failure of the input spiral bevel pinion in the main rotor gearbox, ARL have analyzed the routine recordings of the gearbox vibration which were made by the RAN before the failure. It has been shown that conventional spectral analysis of the gearbox vibration is unable to give an adequate indication of the presence of the fatigue crack due to the production of low level modulation sidebands over a wide frequency range. These sidebands may not be detected because they can be lost in the background vibration of a complex gearbox. Thus in spite of the successful application of spectral analysis to many simple aircraft accessories, it may be inadequate for the detection of cracks in complex gearboxes.

It has also been shown that an alternative technique of vibration analysis called signal averaging can give clear evidence of an abnormality in the gearbox as early as 42 hours before failure. Enhancement of the signal average by digital signal processing using a computer reveals evidence of an abnormality as early as 103 hours before failure. It has been demonstrated that the condition of the gear can be assessed on a GO/NOGO basis using the kurtosis of the enhanced signal average.

The enhancement technique has been developed further to show that it is the phase modulation of the gear meshing vibration which gives the first indication of the presence of the crack, apparently because the crack reduces the local stiffness of the gear allowing the teeth to deflect under load causing a phase lag in the vibration produced. For an early fatigue crack the amplitude modulation is small, demonstrating the inherent unsuitability of many present techniques designed to assess the condition of the gear from the original signal average because these techniques are based on the detection of amplitude modulation.

It has been shown that for an advanced fatigue crack a transient vibration may occur with each gear revolution caused by impulsive loading of the gear as the cracked part deflects. The impacts between gear teeth are independent of the tooth meshing vibration thus making it possible to detect an early fatigue crack by the phase lag in the meshing vibration and an advanced fatigue crack by the impacts which may be produced.

The techniques described are suitable for routine application to helicopter gearboxes, not only to the input spiral bevel pinion in the Wessex gearbox but in principle to other gears in the Wessex and also in other aircraft. The use of these techniques should help to prevent another failure of this type and contribute to improvements in the safety of aircraft operation.

REFERENCES

- [1]. Goldsmith, N. T.—Personal Communication, Aeronautical Research Laboratories, 1984.
- [2]. McFadden, P. D.—“The Application of Vibration Analysis to the Condition Monitoring of Helicopter Gearboxes”, Symposium on Maintenance for the 80s, Institution of Engineers Australia, Sydney, November 4-5, 1980.
- [3]. Edwards, D. H., King, C. N., and Pavia, R. V.—“Vibration Measurement of Accessory Angle Drive Gearboxes on Atar 09C Engines”, Aeronautical Research Laboratories, Mechanical Engineering Report 144, November 1974.
- [4]. Royal Australian Air Force—“F111C TF30 Engine Exhaust Nozzle Control Pumps Engineering Investigation”, HQSC 2612/44.70-D Pt 4, (Restricted), November, 1975.
- [5]. McFadden, P. D.—“Investigation into the Vibration of the Starter Gearbox of an Aircraft Turbine Engine”, Fifth International Symposium on Air Breathing Engines, Bangalore, India, February 16-21, 1981.
- [6]. McFadden, P. D., and Edwards, D. H.—“Vibration Test Procedures for Accessory Angle Drive Gearboxes on Atar 09C Engines, Aeronautical Research Laboratories, Mechanical Engineering Technical Memorandum 408, March 1981.
- [7]. McFadden, P. D., and Smith, J. D.—“Effects of Transmission Path on Measured Gear Vibration”, Transactions of the ASME, Journal of Vibration Acoustics Stress and Reliability in Design, to be published.
- [8]. Randall, R. B.—“Application of B and K Equipment to Frequency Analysis”, Bruel and Kjaer, 2nd edition, September, 1977.
- [9]. Brigham, E. O.—“The Fast Fourier Transform”, Prentice Hall, New Jersey, 1974.
- [10]. Harris, F. J.—“On the Use of Windows for Harmonic Analysis with the Discrete Fourier Transform”, Proceedings of the IEEE, vol. 166, no. 1, pp 51-83, January, 1978.
- [11]. Nuttall, A. H.—“Some Windows with Very Good Sidelobe Behaviour”, IEEE Transactions on Acoustics Speech and Signal Processing, vol. ASSP-29, no. 1, pp 84-91, February, 1981.
- [12]. Cox, R. G.—“Window Functions for Spectrum Analysis”, Hewlett Packard Journal, pp 10-11, September, 1978.
- [13]. Oppenheim, A. V., and Schafer, R. W.—“Digital Signal Processing”, Prentice-Hall, New Jersey, chapter 10, 1975.
- [14]. Randall, R. B.—“A New Method of Modelling Gear Faults”, Transactions of the ASME, Journal of Mechanical Design, vol. 104, pp 259-267, April, 1982.
- [15]. McFadden, P. D.—“Cepstrum Analysis of Gear Vibration”, in course of preparation.

- [16]. Braun, S.—"The Extraction of Periodic Waveforms by Time Domain Averaging", *Acustica*, vol. 32, pp 69-77, 1975.
- [17]. McFadden, P. D.—"A Phase-Locked Frequency Multiplier for the Signal Averaging of the Vibration of the Wessex Helicopter Input Spiral Bevel Pinion", Aeronautical Research Laboratories, Aero Propulsion Technical Memorandum 423, January, 1985.
- [18]. McFadden, P. D.—"Proposal for Modifications to the Wessex Helicopter Main Rotor Gearbox Vibration Monitoring Program", Aeronautical Research Laboratories, Aero Propulsion Technical Memorandum 422, January 1985.
- [19]. Stewart, R. M.—"Some Useful Data Analysis Techniques for Gearbox Diagnostics", Machinery Health Monitoring Group, Institute of Sound and Vibration Research, University of Southampton, Report MHM/R/10/77, July 1977.
- [20]. Croxton, F. E., and Cowden, D. J.—"Applied General Statistics", Pitman, chapter 10, 1962.
- [21]. Dyer, D., and Stewart, R. M.—"Detection of Rolling Element Bearing Damage by Statistical Vibration Analysis", *Transactions of the ASME, Journal of Mechanical Design*, vol. 100, pp 229-235, April 1978.
- [22]. McFadden, P. D., and Smith, J. D.—"A Signal Processing Technique for Detecting Local Defects in a Gear from the Signal Average of the Vibration", *Proceedings of the Institution of Mechanical Engineers*, vol. 199, part C, no. 4, 1985.
- [23]. Bracewell, R. N. "The Fourier Transform and its Applications", McGraw-Hill Kogakusha, pp 267-272, 2nd edition, 1978.
- [24]. McFadden, P. D. "Detecting Fatigue Cracks in Gears by Amplitude and Phase Demodulation of the Meshing Vibration", *Transactions of the ASME, Journal of Vibration Acoustics Stress and Reliability in Design*, to be published.
- [25]. Stewart, R. M. —"The Development of Multi-Level Diagnostics for Rotating Machinery", Machinery Health Monitoring Group, Institute of Sound and Vibration Research, University of Southampton, Report MHM R 08/79, August 1979.
- [26]. Board, D. B. - "Incipient Failure Detection for Helicopter Drive Trains", AIAA/SAE 13th Propulsion Conference, Orlando, Florida, Paper 77-898, July 11-13, 1977.
- [27]. McFadden, P. D. "Low Frequency Vibration Generated by Gear Tooth Impacts", *NDT International*, vol. 18, no. 5, pp 279-282, October 1985.
- [28]. Cameron, B. G., and Stuckey, M. J. Personal Communication, Westland Helicopters Ltd, Mechanical Research Department.
- [29]. Carlson, A. B. "Communication Systems", McGraw Hill, pp 181-183, 240-241, 1975.

APPENDIX

When a carrier $X_m \cos(2\pi m f_x t + \phi_m)$ is amplitude modulated by a function $a_m(t)$, the resulting signal $z_m(t)$ is given by [29]:

$$z_m(t) = (1 + a_m(t)) X_m \cos(2\pi m f_x t + \phi_m)$$

When the carrier is phase modulated by $b_m(t)$, the resulting signal is given by [29]:

$$\begin{aligned} z_m(t) &= X_m \cos(2\pi m f_x t + \phi_m + b_m(t)) \\ &= X_m [\cos(2\pi m f_x t + \phi_m) \cos(b_m(t)) - \sin(2\pi m f_x t + \phi_m) \sin(b_m(t))] \end{aligned}$$

If $b_m(t) \ll \pi$, small angle approximations can be applied [29] giving:

$$z_m(t) \simeq X_m [\cos(2\pi m f_x t + \phi_m) - b_m(t) \sin(2\pi m f_x t + \phi_m)]$$

When simultaneous amplitude and phase modulation occur, the resulting signal is given by:

$$z_m(t) \simeq X_m (1 + a_m(t)) [\cos(2\pi m f_x t + \phi_m) - b_m(t) \sin(2\pi m f_x t + \phi_m)]$$

If $a_m(t), b_m(t) \ll 1$, this reduces to

$$\begin{aligned} z_m(t) &\simeq X_m [\cos(2\pi m f_x t + \phi_m) \\ &\quad + a_m(t) \cos(2\pi m f_x t + \phi_m) - b_m(t) \sin(2\pi m f_x t + \phi_m)] \end{aligned}$$

LIST OF FIGURES

- Figure 1. Piece of the failed Wessex input spiral bevel pinion.
- Figure 2. Path of the fatigue crack in the pinion.
- Figure 3. Possible time history of the crack area [1].
- Figure 4. Possible time history of the crack front [1].
- Figure 5. Vibration spectrum of a jet engine accessory gearbox.
- Figure 6. Modulation sidebands caused by gear eccentricity.
- Figure 7. Modulation sidebands caused by a gear crack.
- Figure 8. Spectrum of a sinusoid.
Block length = 50.5 periods. No weighting.
- Figure 9. Spectrum of a sinusoid.
Block length = 50.5 periods. Hanning weighting.
- Figure 10. Spectrum of a sinusoid.
Block length = 50.5 periods. Blackman-Harris weighting.
- Figure 11. Spectrum of gearbox WAK143.
42 hours before failure.
Calculated by HP3582A analyzer.
- Figure 12. Spectrum of gearbox WAK143.
42 hours before failure.
Calculated by SD335 analyzer.
- Figure 13. Spectrum of gearbox WAL189.
Calculated by SD335 analyzer.
- Figure 14. Equipment required for signal averaging.
- Figure 15. Extraction of a sinusoid from random noise.
- Figure 16. Pass band shape of a comb filter.
- Figure 17. Block diagram of a phase-locked frequency multiplier.
- Figure 18. Spectrum of gearbox WAK143 after band pass filtering.
- Figure 19. Signal average of input pinion of gearbox WAK143.
42 hours before failure.
- Figure 20. Signal average of input pinion of gearbox WAM284.
- Figure 21. Signal average of input pinion of gearbox WAK143.
103 hours before failure.
- Figure 22. Spectrum of signal average of input pinion of gearbox WAK143.
103 hours before failure.
- Figure 23. Signal average of input pinion of gearbox WAK143.
103 hours before failure.
Meshing harmonics eliminated.

- Figure 24.—Signal average of input pinion of gearbox WAK143.
103 hours before failure.
Meshing harmonics and ghost eliminated.
- Figure 25.—Signal average of input pinion of gearbox WAK143.
103 hours before failure.
Band pass filtered 30 to 58 shaft orders.
- Figure 26.—Signal average of input pinion of gearbox WAK143.
103 hours before failure.
Band pass filtered 30 to 58 shaft orders.
Meshing harmonic at 44 shaft orders eliminated.
- Figure 27.—Complex rotating vector and its projections.
- Figure 28.—Signal average of input pinion of gearbox WAK143.
103 hours before failure.
Band pass filtered 30 to 58 shaft orders.
Meshing harmonic at 44 shaft orders eliminated.
Enveloped.
- Figure 29.—Amplitude of complex vector.
103 hours before failure.
- Figure 30.—Phase of complex vector.
103 hours before failure.
- Figure 31.—Amplitude of complex vector.
42 hours before failure.
- Figure 32.—Phase of complex vector.
42 hours before failure.
- Figure 33.—Polar plot of complex vector.
103 hours before failure.
- Figure 34.—Polar plot of complex vector.
42 hours before failure.
- Figure 35.—Low frequency spectrum of signal average of input pinion.
of gearbox WAK143.
103 hours before failure.
- Figure 36.—Low frequency spectrum of signal average of input pinion.
of gearbox WAK143.
42 hours before failure.
- Figure 37.—Signal average of input pinion of gearbox WAK143.
103 hours before failure.
Low pass filtered 0 to 18 shaft orders.
- Figure 38.—Signal average of input pinion of gearbox WAK143.
42 hours before failure.
Low pass filtered 0 to 18 shaft orders.



FIG. 1 PIECE OF THE FAILED WESSEX INPUT SPIRAL BEVEL PINION

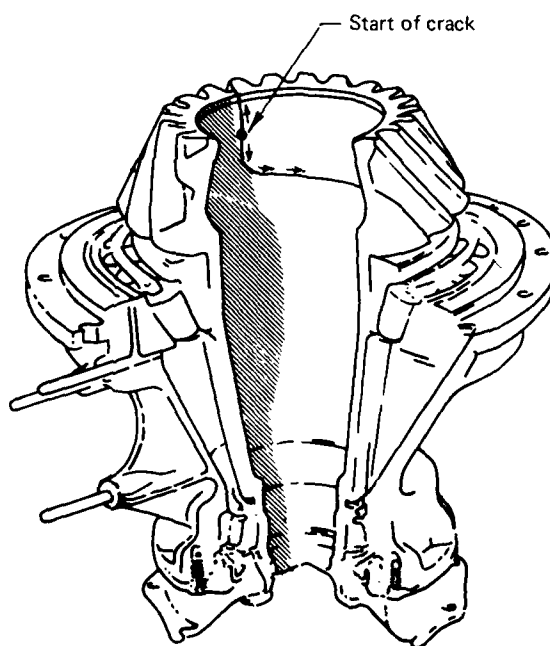


FIG. 2 PATH OF THE FATIGUE CRACK IN THE PINION

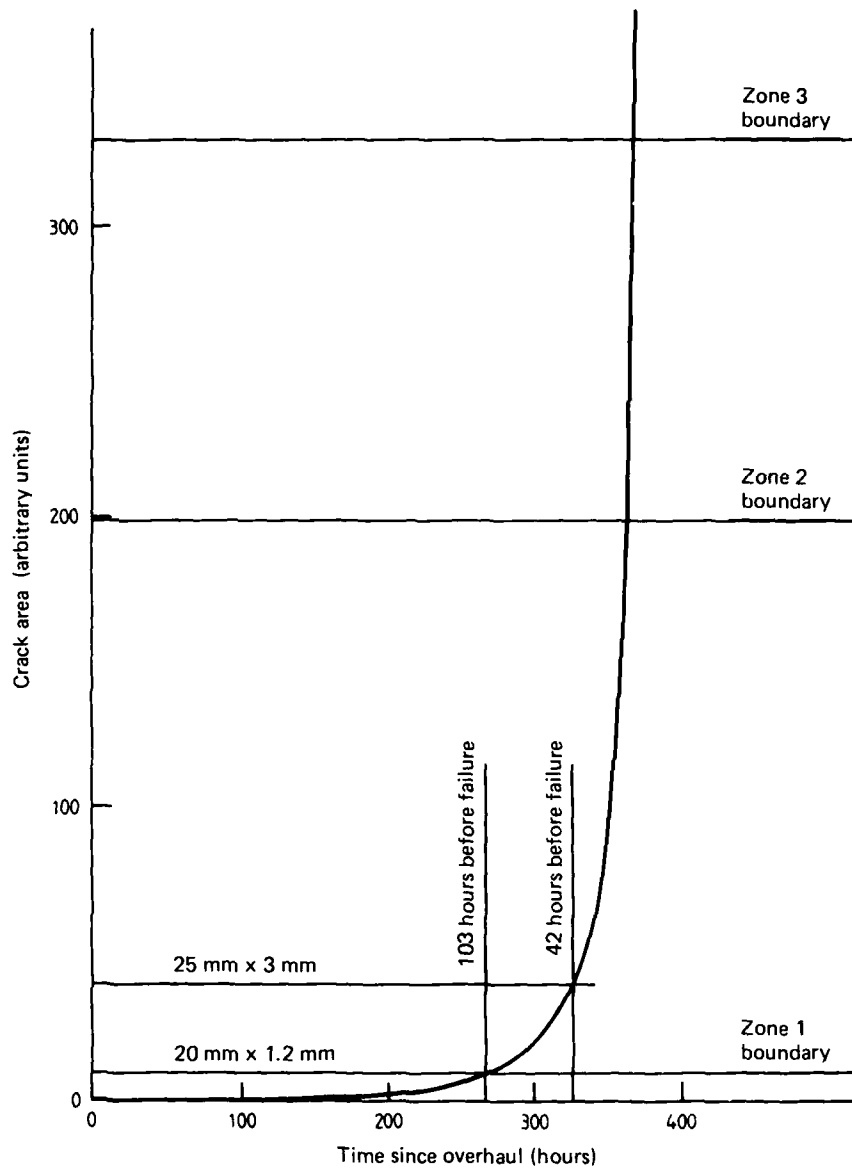


FIG. 3 POSSIBLE TIME HISTORY OF THE CRACK AREA [1]

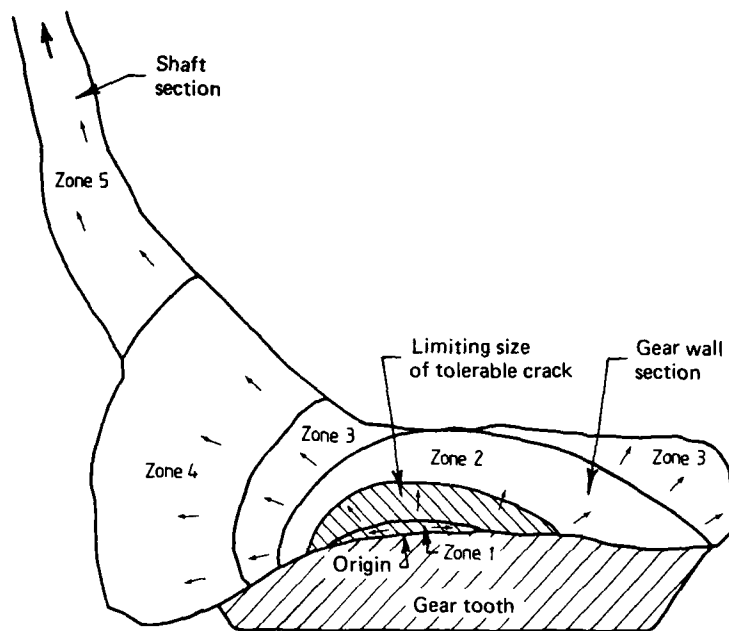


FIG. 4 POSSIBLE TIME HISTORY OF THE CRACK FRONT [1]

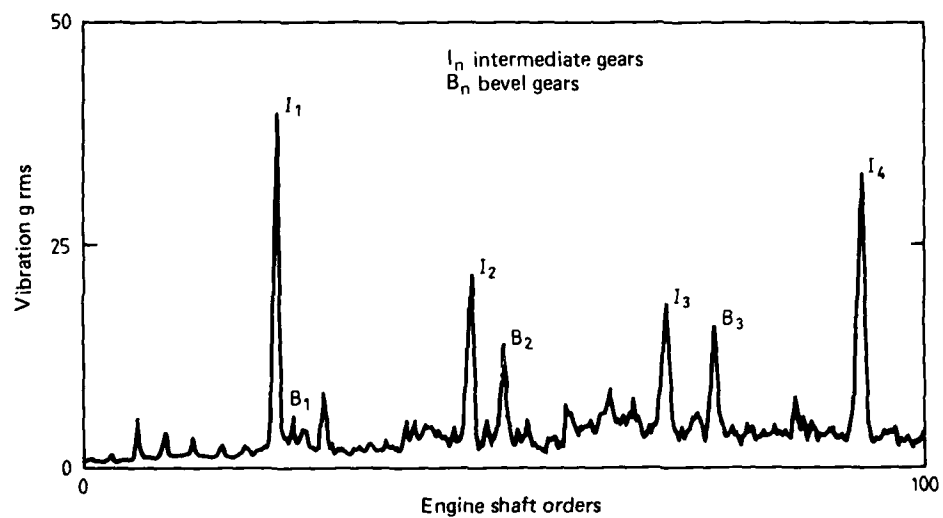


FIG. 5 VIBRATION SPECTRUM OF A JET ENGINE ACCESSORY GEARBOX

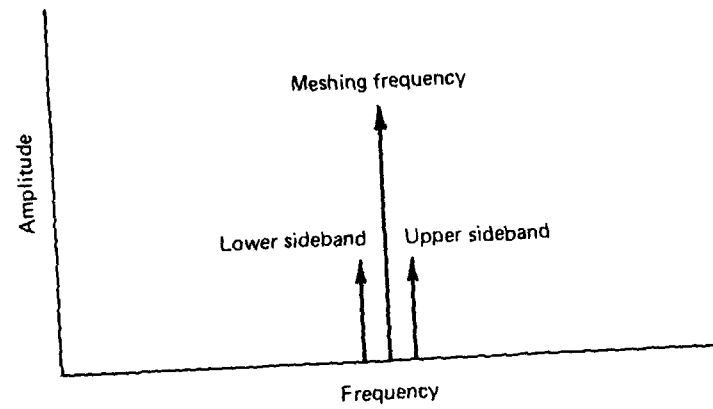


FIG. 6 MODULATION SIDEBANDS CAUSED BY GEAR ECCENTRICITY

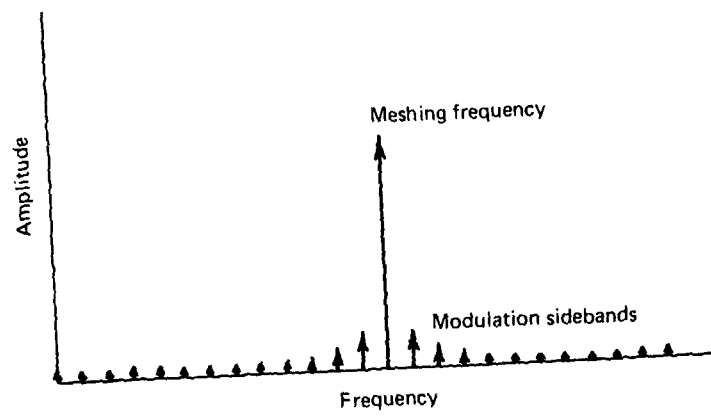


FIG. 7 MODULATION SIDEBANDS CAUSED BY A GEAR CRACK

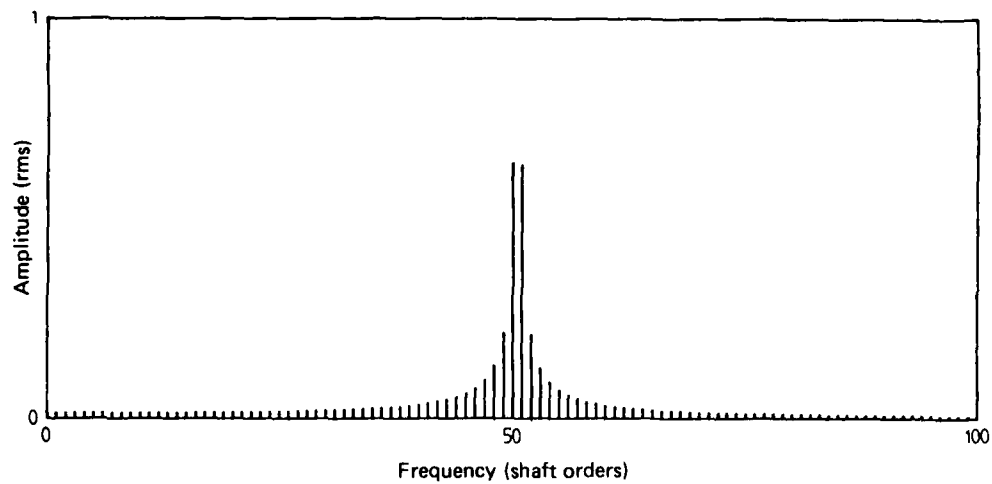


FIG. 8 SPECTRUM OF A SINUSOID
BLOCK LENGTH = 50.5 PERIODS NO WEIGHTING

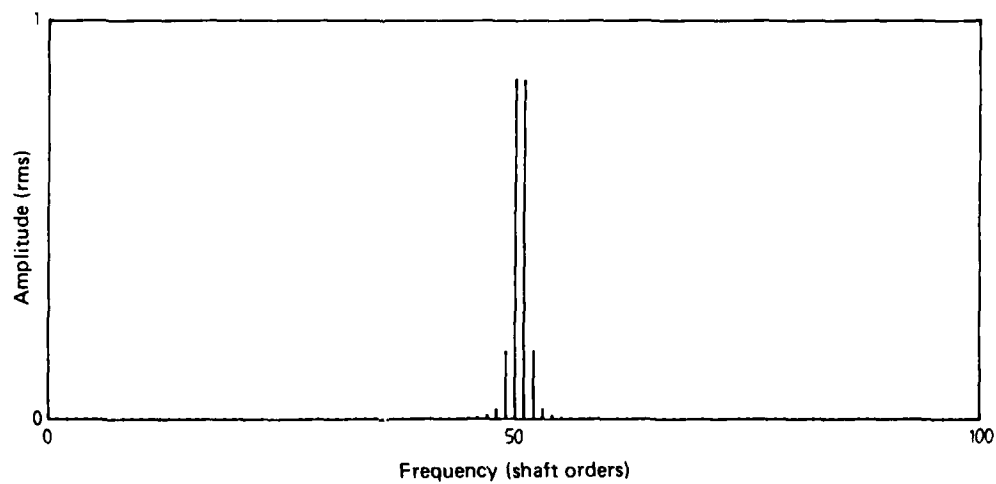


FIG. 9 SPECTRUM OF A SINUSOID
BLOCK LENGTH = 50.5 PERIODS HANNING WEIGHTING

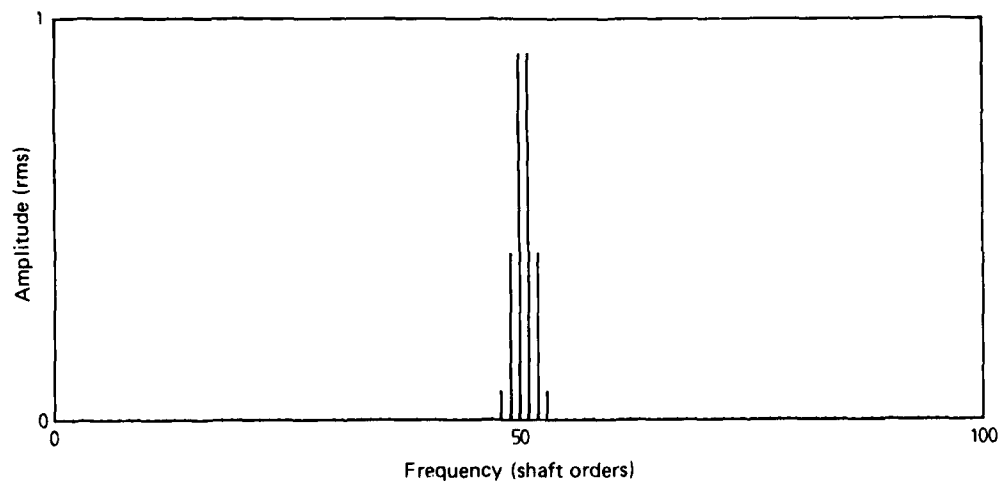


FIG. 10 SPECTRUM OF A SINUSOID
BLOCK LENGTH = 50.5 PERIODS BLACKMAN-HARRIS WEIGHTING

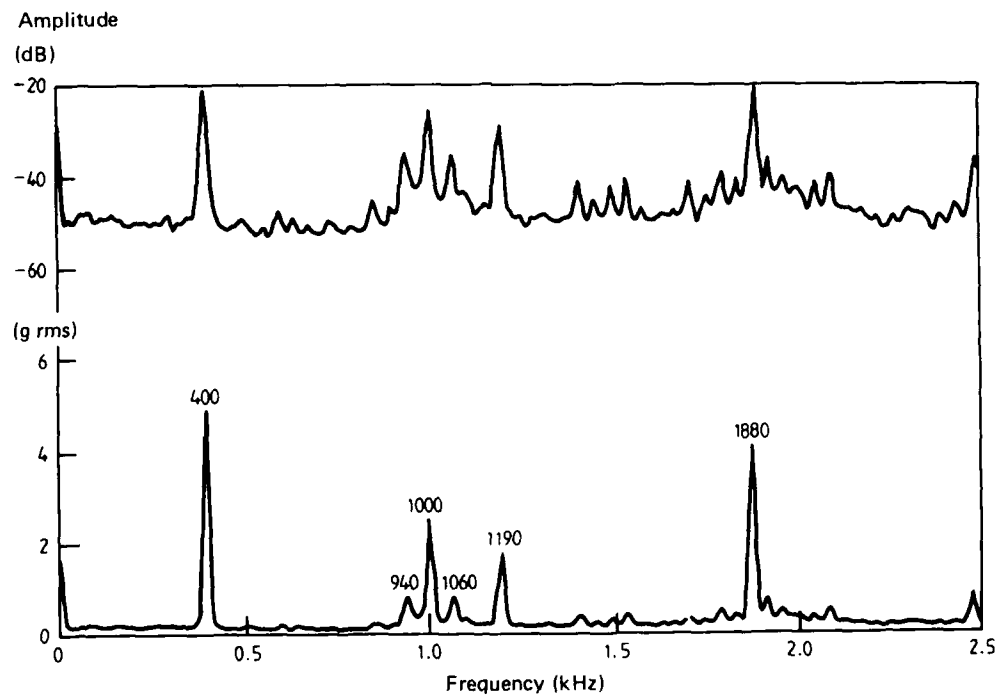


FIG. 11 SPECTRUM OF GEARBOX WAK143
42 HOURS BEFORE FAILURE
CALCULATED BY HP3582A ANALYZER

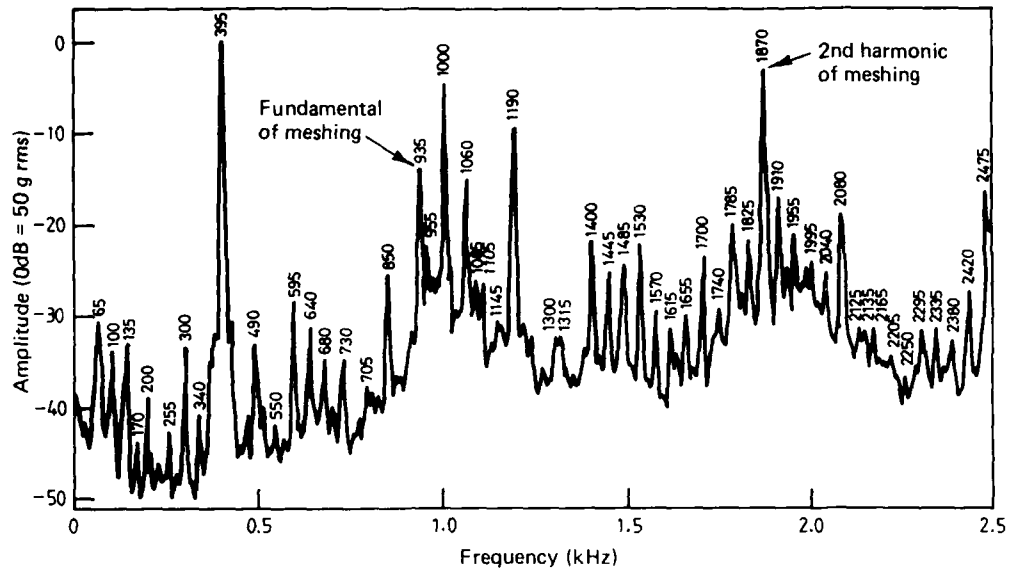


FIG. 12 SPECTRUM OF GEARBOX WAK143
42 HOURS BEFORE FAILURE
CALCULATED BY SD335 ANALYZER

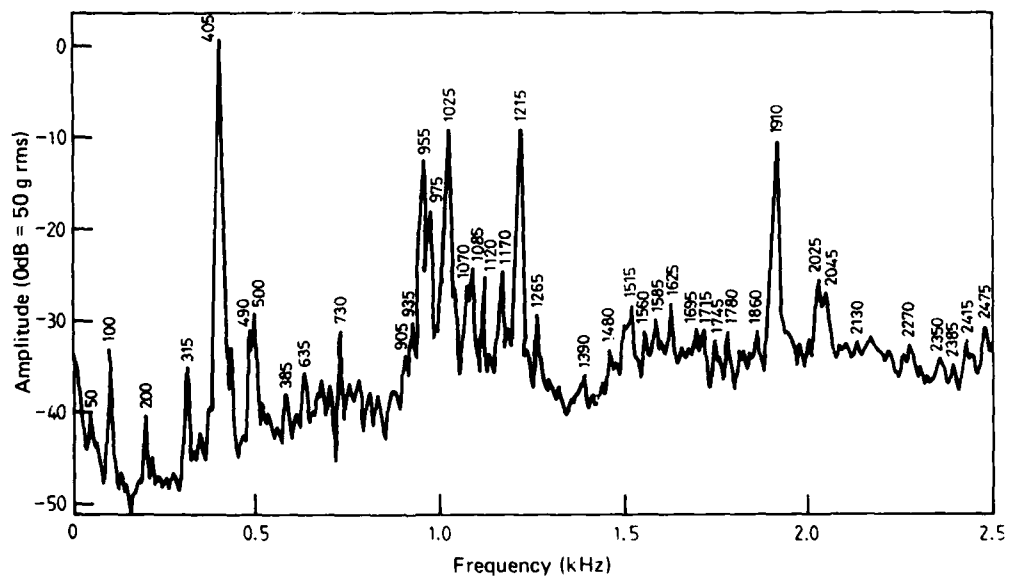


FIG. 13 SPECTRUM OF GEARBOX WAL189
CALCULATED BY SD335 ANALYZER

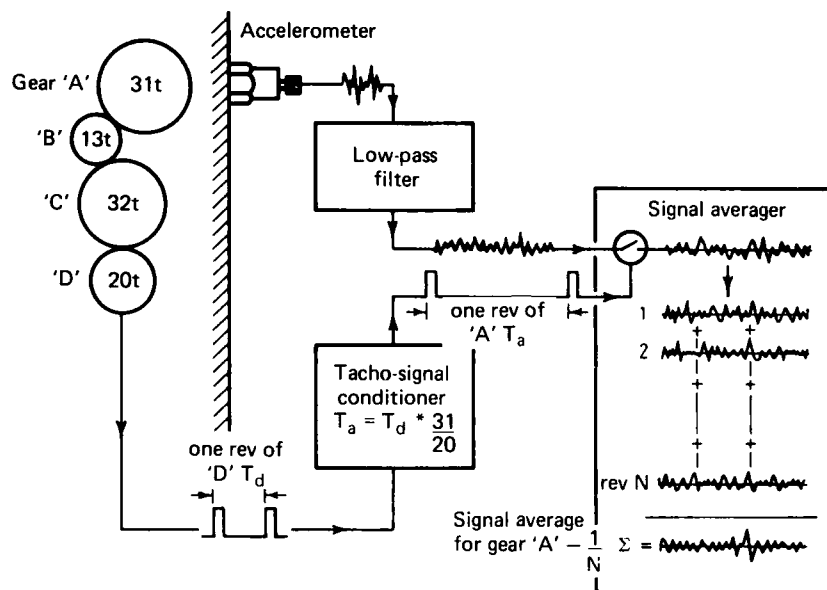


FIG. 14 EQUIPMENT REQUIRED FOR SIGNAL AVERAGING

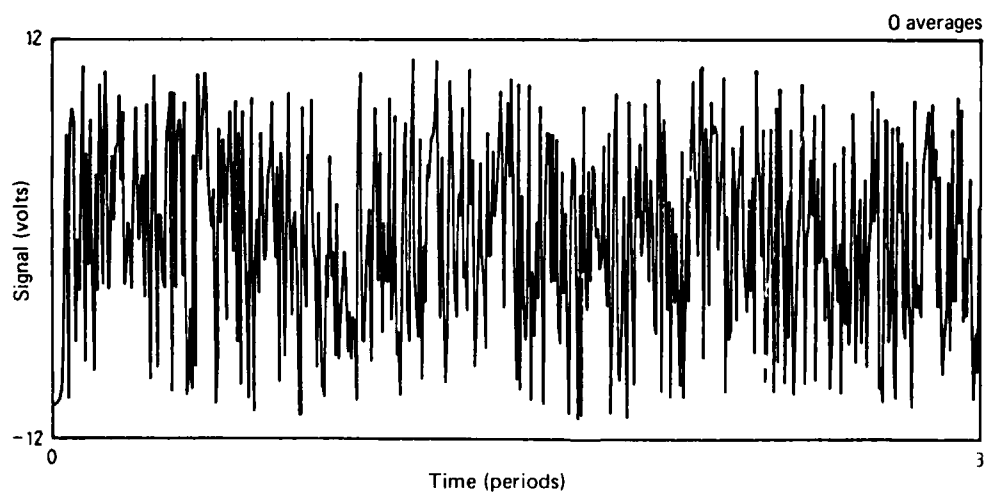


FIG. 15 (a) EXTRACTION OF A SINUSOID FROM RANDOM NOISE

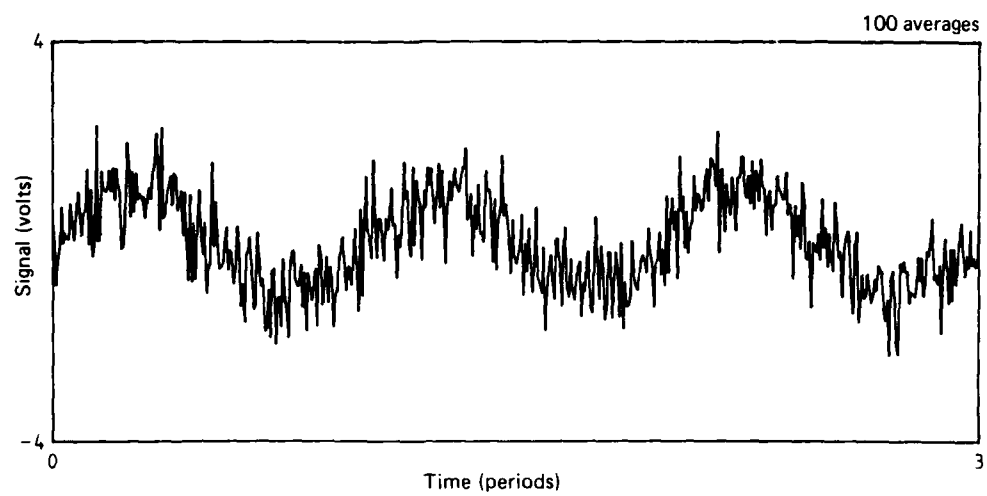


FIG. 15 (b)

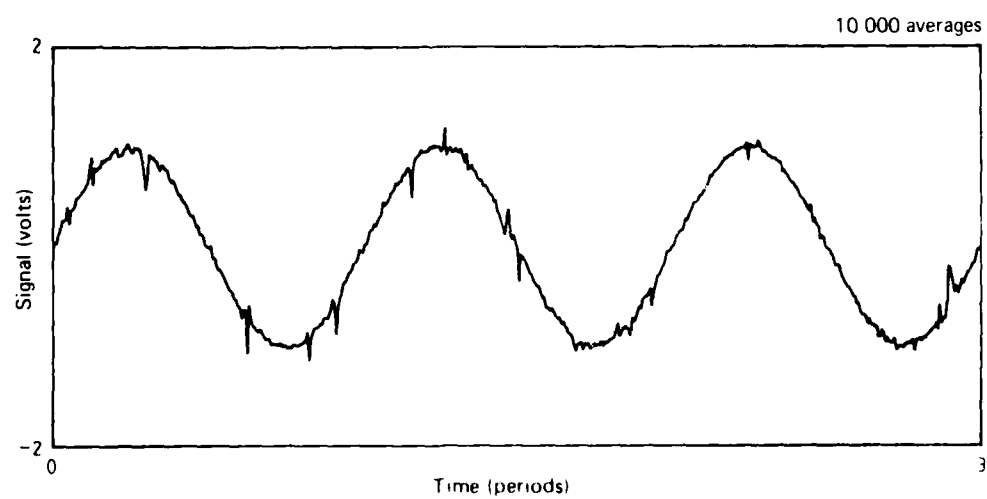


FIG. 15 (c)

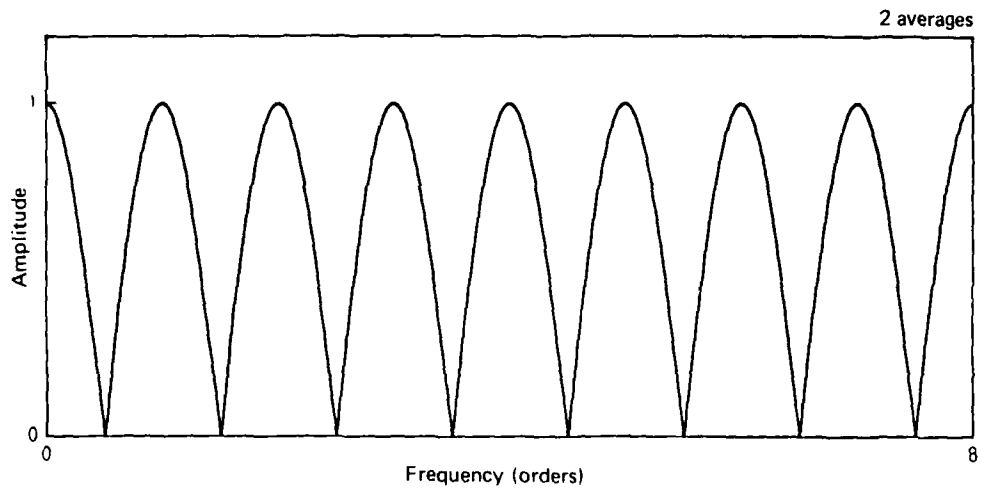


FIG. 16 (a) PASS BAND SHAPE OF A COMB FILTER

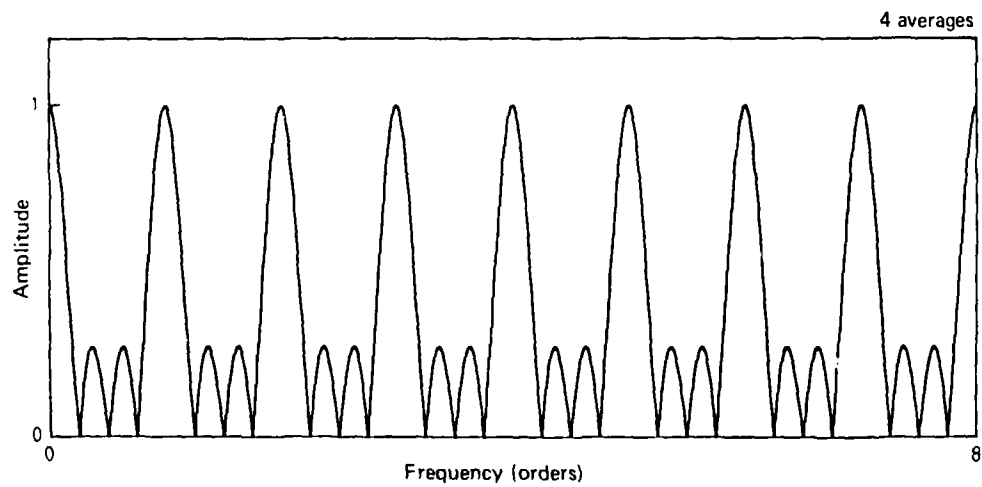


FIG. 16(b)

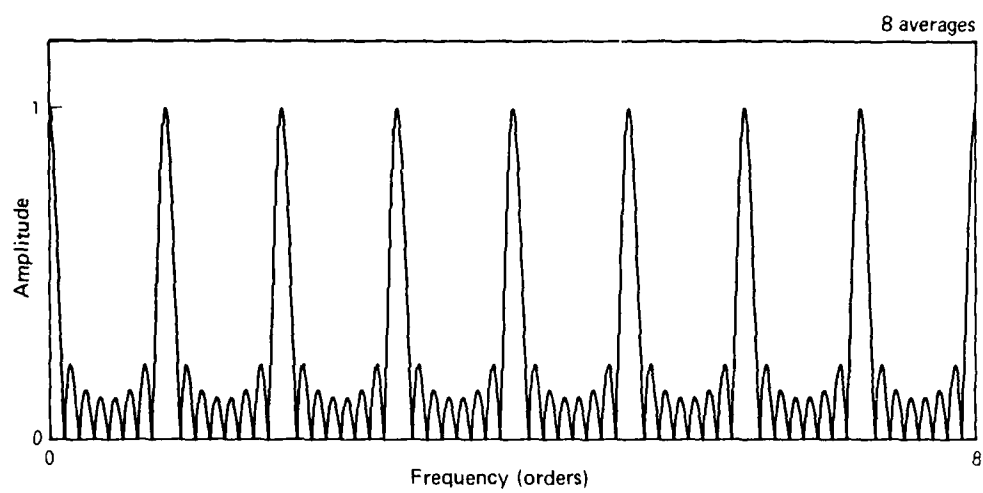


FIG. 16 (c)

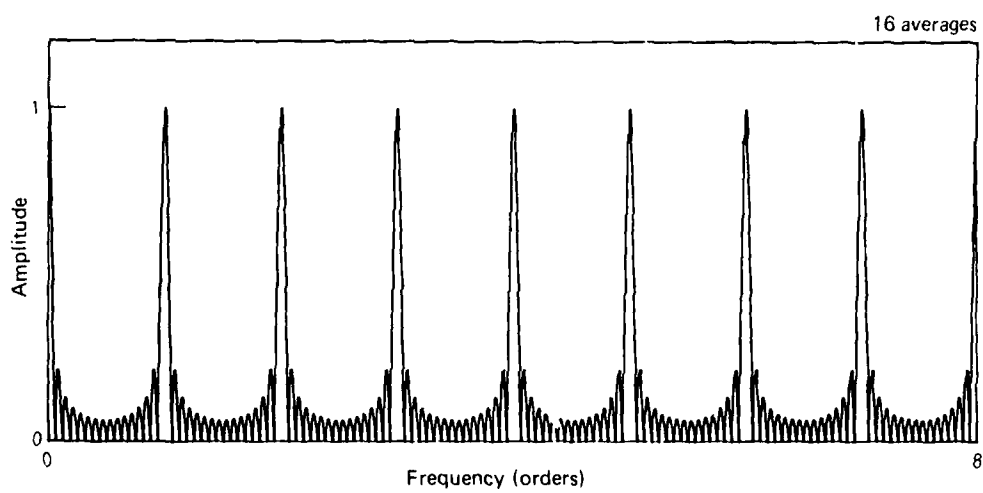


FIG. 16 (d)

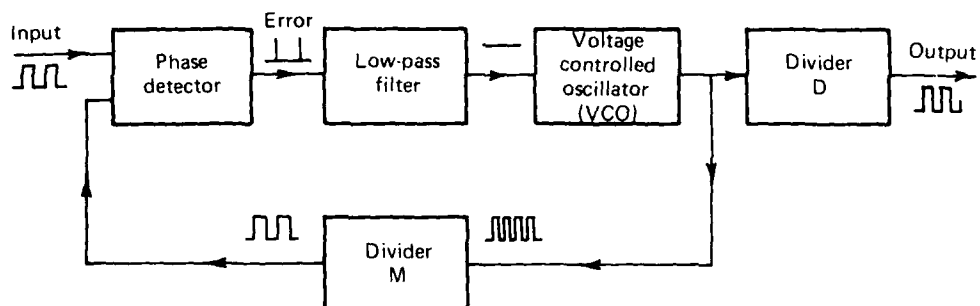


FIG. 17 BLOCK DIAGRAM OF A PHASE-LOCKED FREQUENCY MULTIPLIER

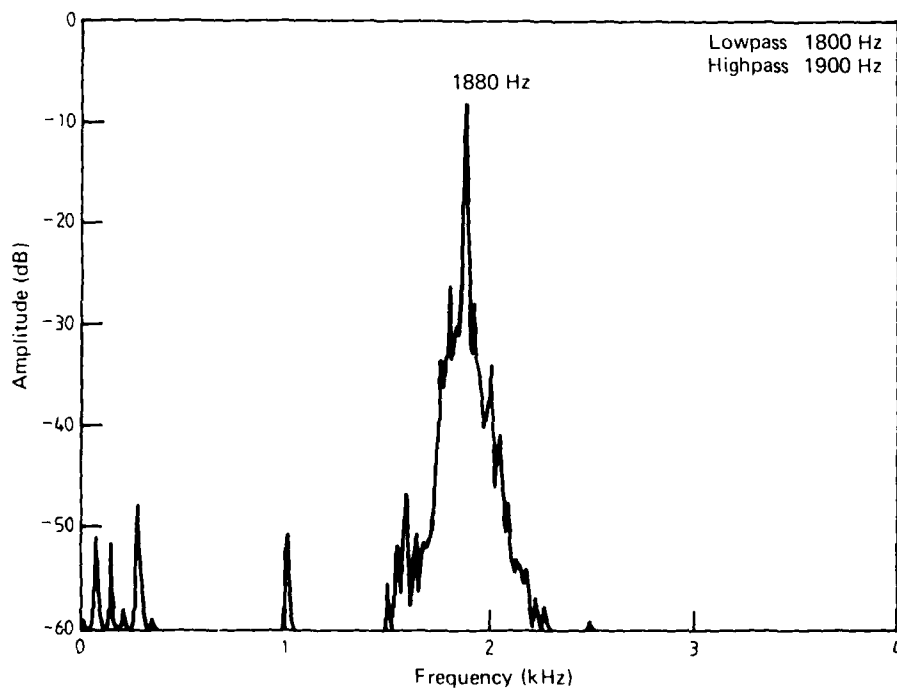


FIG. 18 SPECTRUM OF GEARBOX WAK143 AFTER BAND PASS FILTERING

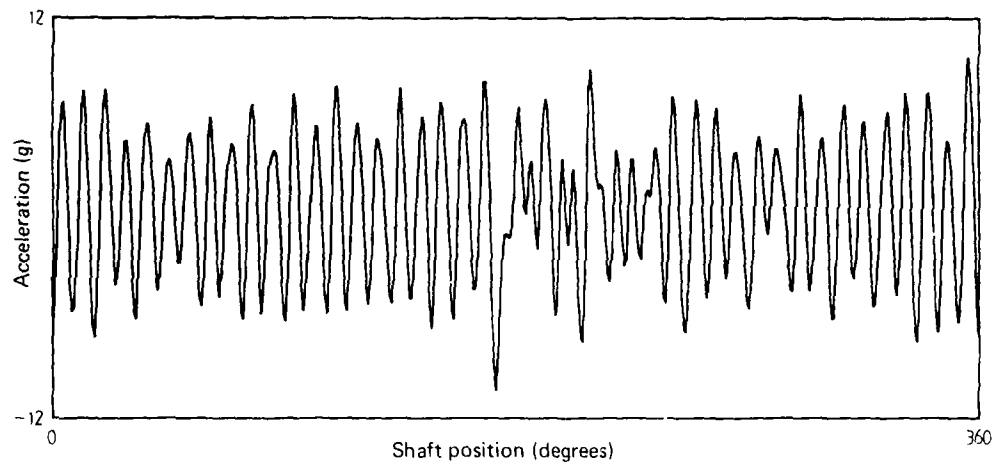


FIG. 19 SIGNAL AVERAGE OF INPUT PINION OF GEARBOX WAK143
42 HOURS BEFORE FAILURE

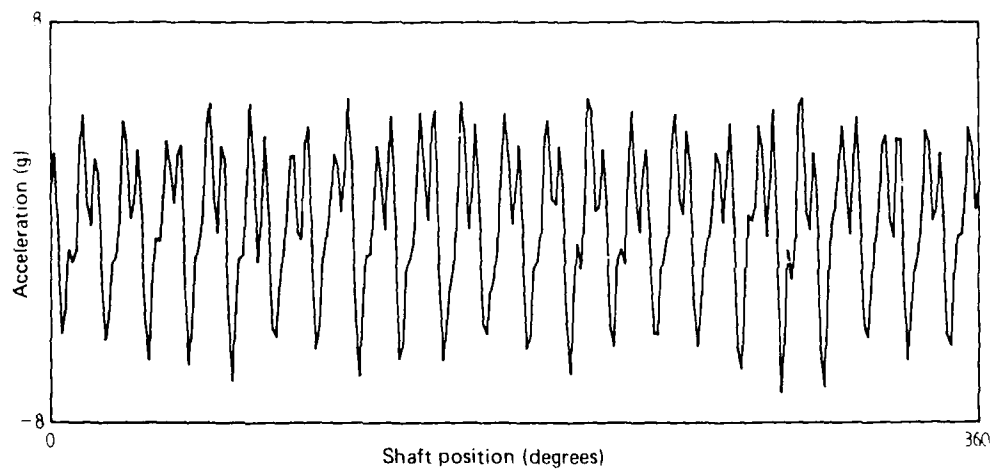


FIG. 20 SIGNAL AVERAGE OF INPUT PINION OF GEARBOX WAM284

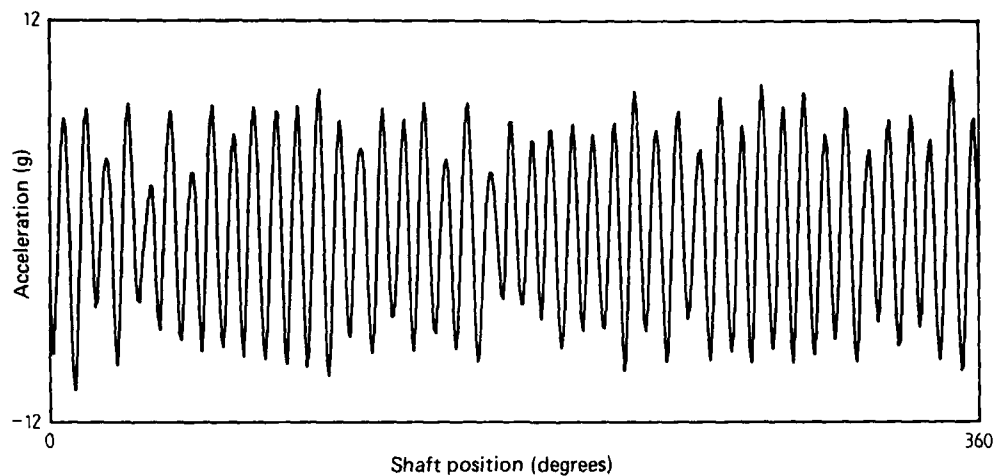


FIG. 21 SIGNAL AVERAGE OF INPUT PINION OF GEARBOX WAK143
103 HOURS BEFORE FAILURE

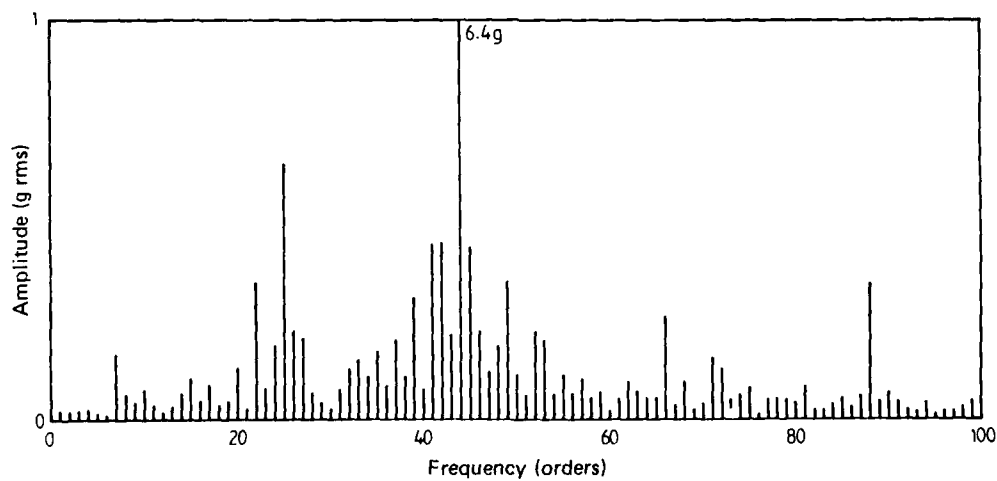


FIG. 22 SPECTRUM OF SIGNAL AVERAGE OF INPUT PINION OF GEARBOX WAK143
103 HOURS BEFORE FAILURE

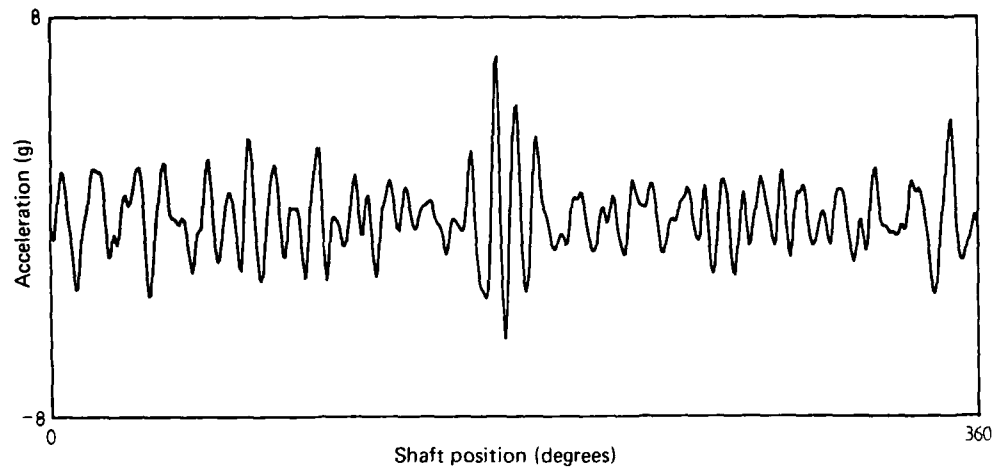


FIG. 23 SIGNAL AVERAGE OF INPUT PINION OF GEARBOX WAK143
103 HOURS BEFORE FAILURE
MESHING HARMONICS ELIMINATED

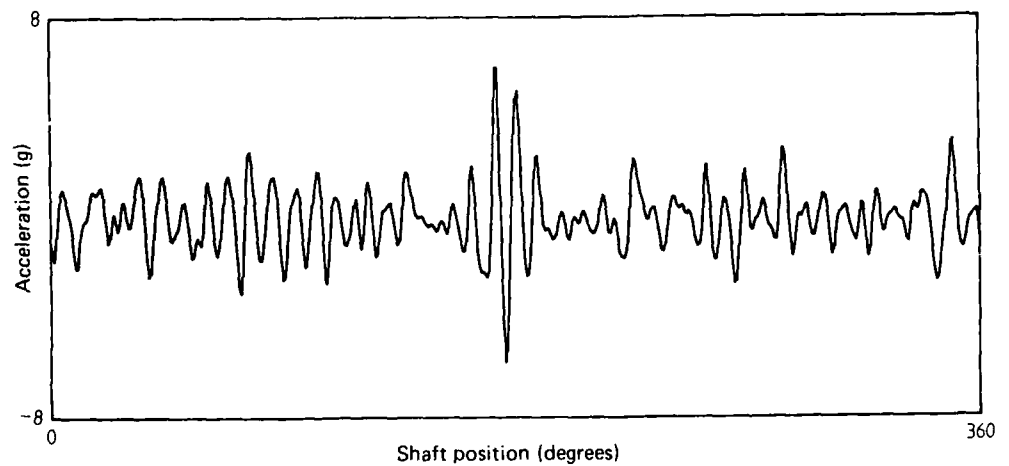


FIG. 24 SIGNAL AVERAGE OF INPUT PINION OF GEARBOX WAK143
103 HOURS BEFORE FAILURE
MESHING HARMONICS AND GHOST ELIMINATED

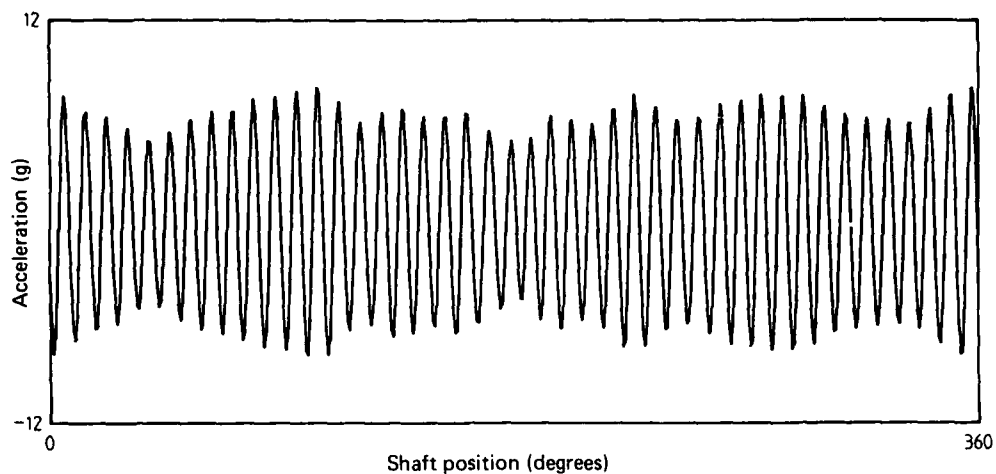


FIG. 25 SIGNAL AVERAGE OF INPUT PINION OF GEARBOX WAK143
103 HOURS BEFORE FAILURE
BAND PASS FILTERED 30 TO 58 SHAFT ORDERS

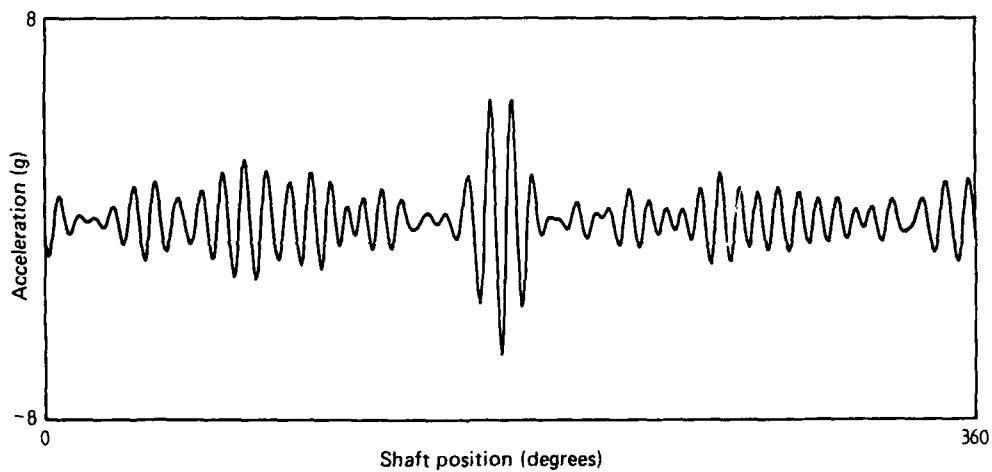


FIG. 26 SIGNAL AVERAGE OF INPUT PINION OF GEARBOX WAK143
103 HOURS BEFORE FAILURE
BAND PASS FILTERED 30 TO 58 SHAFT ORDERS
MESHING HARMONIC AT 44 SHAFT ORDERS ELIMINATED

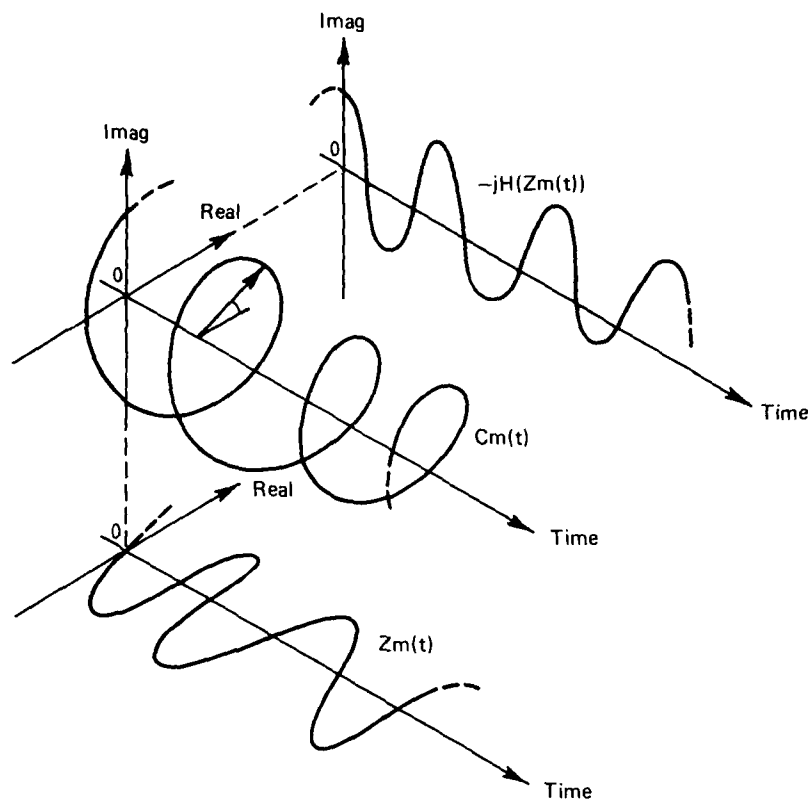


FIG. 27 COMPLEX ROTATING VECTOR AND ITS PROJECTIONS

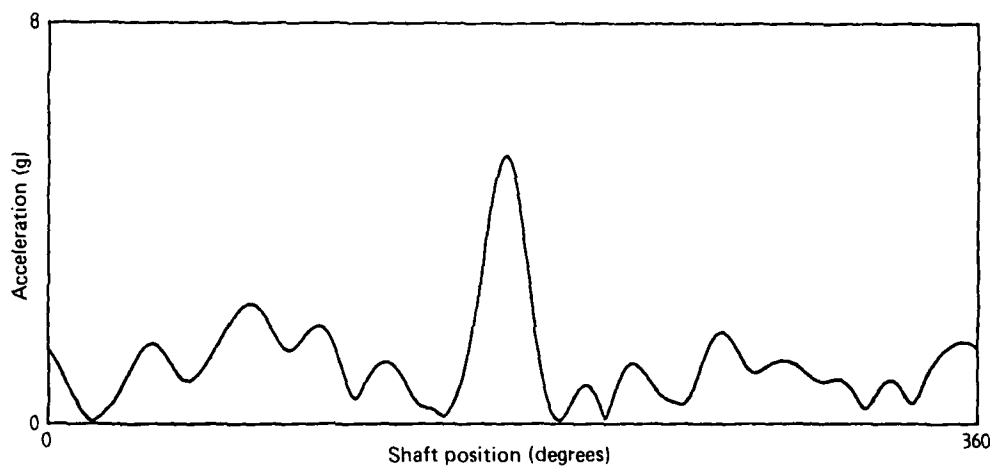


FIG. 28 SIGNAL AVERAGE OF INPUT PINION OF GEARBOX WAK143
103 HOURS BEFORE FAILURE
BAND PASS FILTERED 30 TO 58 SHAFT ORDERS
MESHING HARMONIC AT 44 SHAFT ORDERS ELIMINATED
ENVELOPED

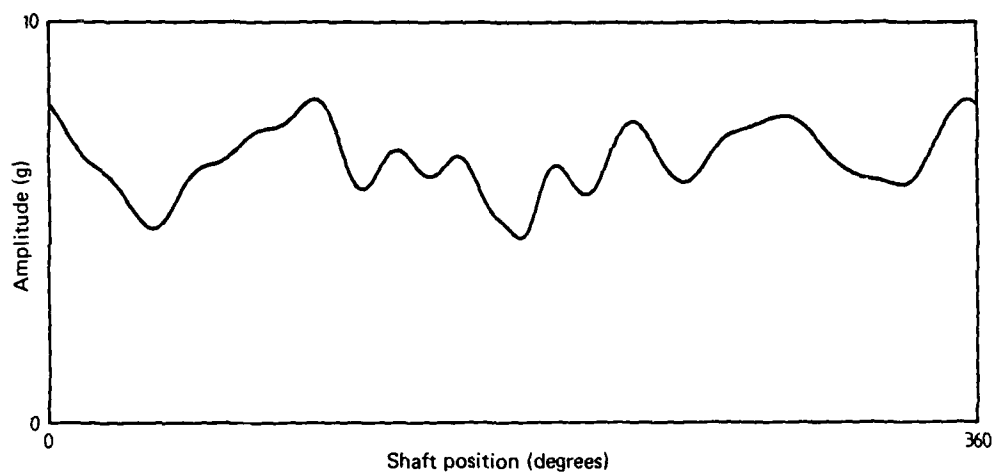


FIG. 29 AMPLITUDE OF COMPLEX VECTOR
103 HOURS BEFORE FAILURE

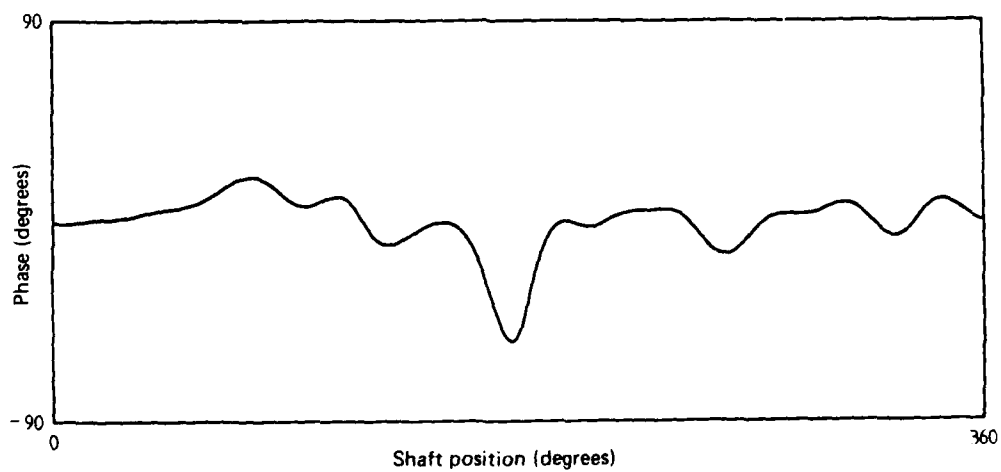


FIG. 30 PHASE OF COMPLEX VECTOR
103 HOURS BEFORE FAILURE

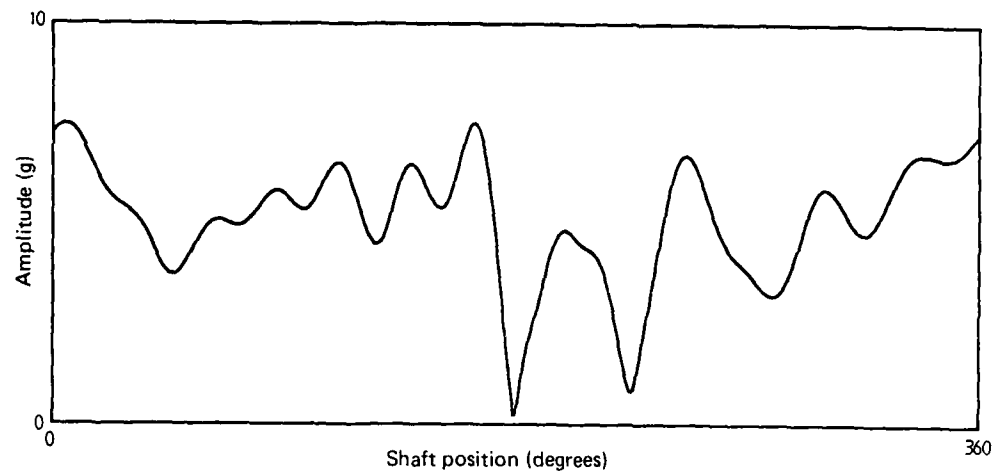


FIG. 31 AMPLITUDE OF COMPLEX VECTOR
42 HOURS BEFORE FAILURE

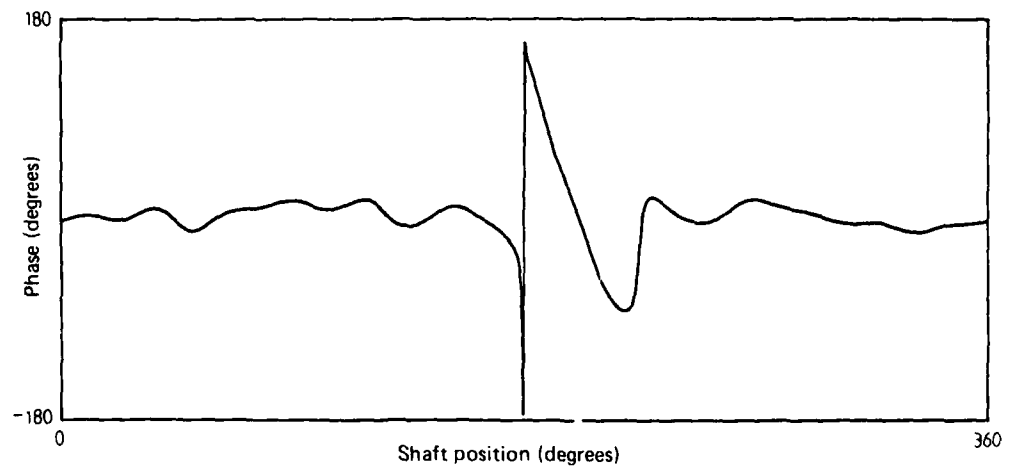


FIG. 32 PHASE OF COMPLEX VECTOR
42 HOURS BEFORE FAILURE

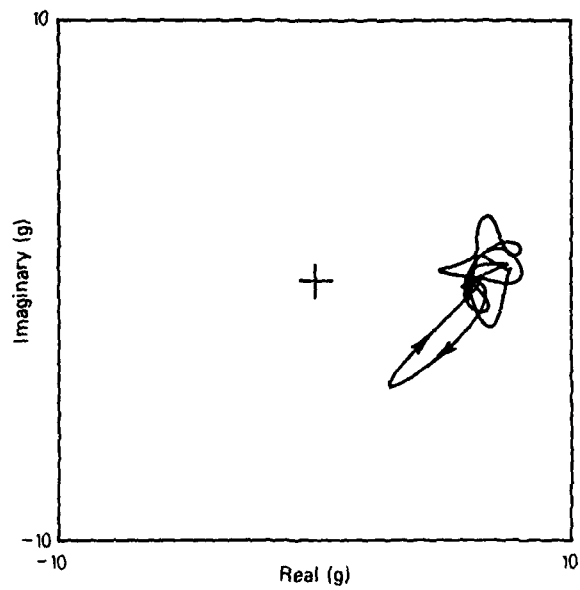


FIG. 33 POLAR PLOT OF COMPLEX VECTOR
103 HOURS BEFORE FAILURE

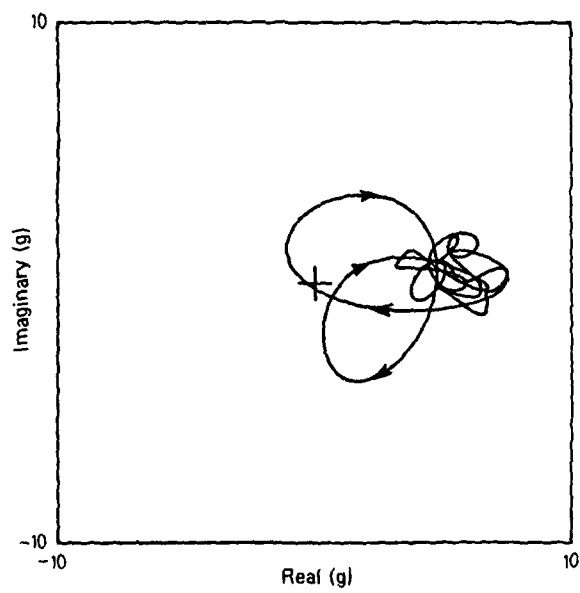


FIG. 34 POLAR PLOT OF COMPLEX VECTOR
42 HOURS BEFORE FAILURE

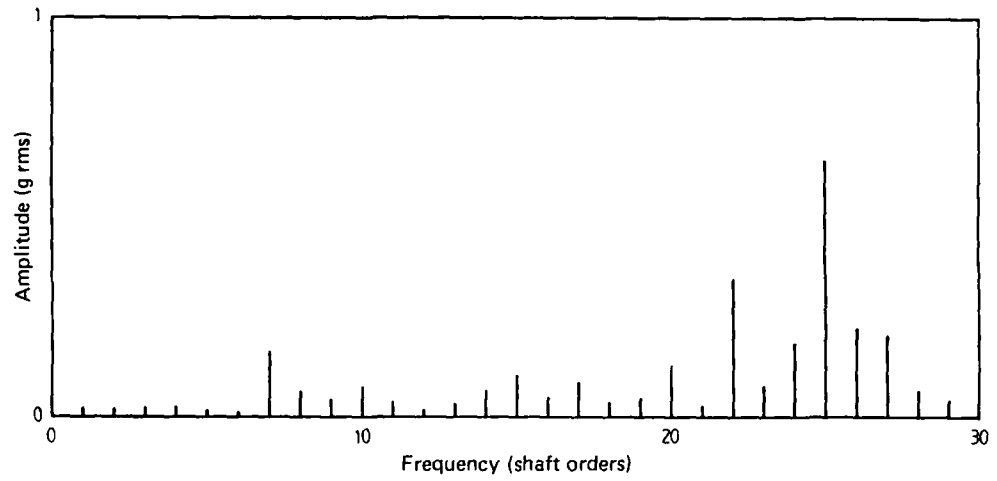


FIG. 35 LOW FREQUENCY SPECTRUM OF SIGNAL AVERAGE OF INPUT PINION
OF GEARBOX WAK143
103 HOURS BEFORE FAILURE

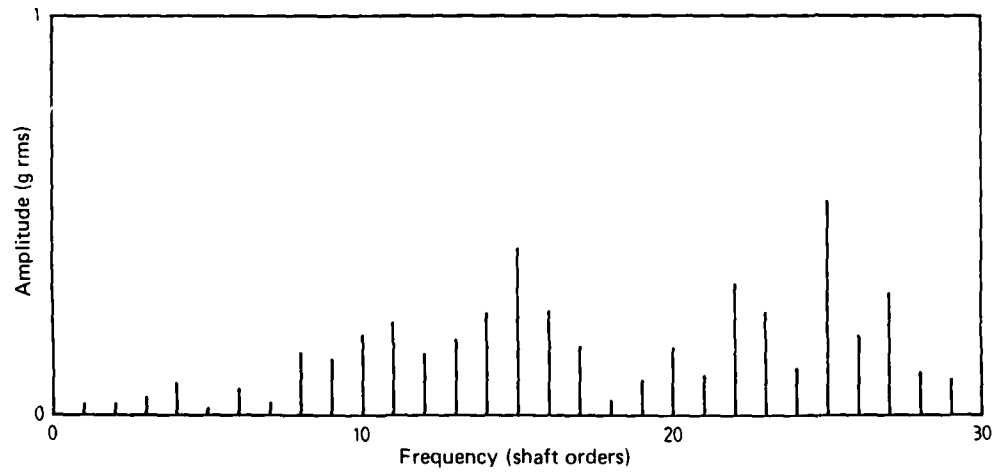


FIG. 36 LOW FREQUENCY SPECTRUM OF SIGNAL AVERAGE OF INPUT PINION
OF GEARBOX WAK143
42 HOURS BEFORE FAILURE

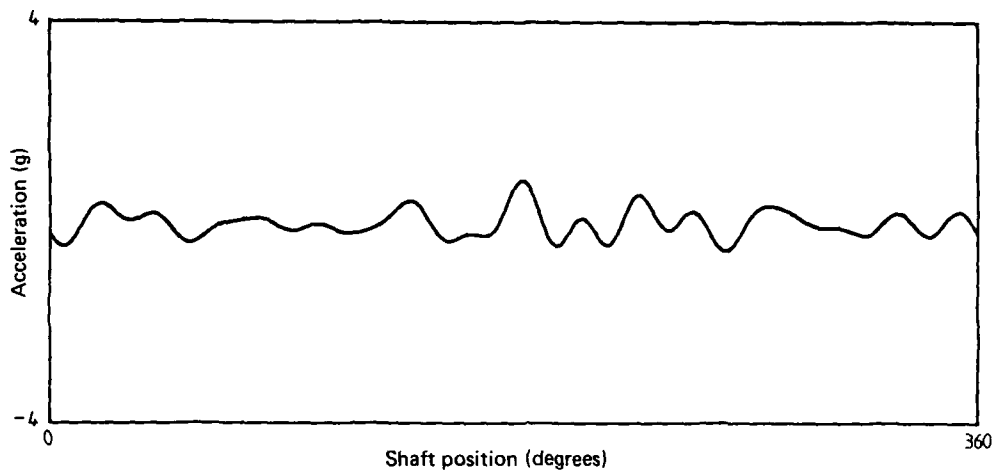


FIG. 37 SIGNAL AVERAGE OF INPUT PINION OF GEARBOX WAK143
103 HOURS BEFORE FAILURE
LOW PASS FILTERED 0 TO 18 SHAFT ORDERS

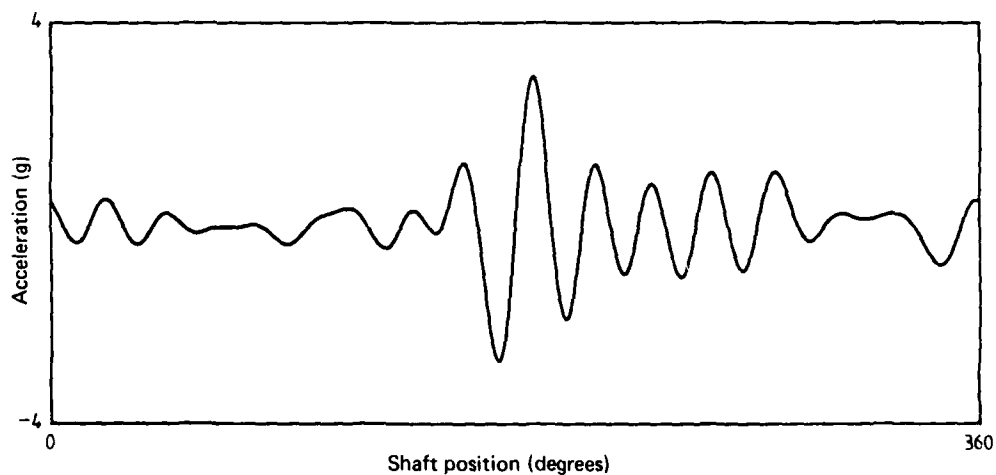


FIG. 38 SIGNAL AVERAGE OF INPUT PINION OF GEARBOX WAK143
42 HOURS BEFORE FAILURE
LOW PASS FILTERED 0 TO 18 SHAFT ORDERS

DISTRIBUTION

AUSTRALIA

DEPARTMENT OF DEFENCE

Defence Central

Chief Defence Scientist
Deputy Chief Defence Scientist
Superintendent, Science and Program Administration
Controller, External Relations, Projects and Analytical Studies
Defence Science Adviser (UK) (Doc. Data sheet only)
Counsellor, Defence Science (USA) (Doc. Data sheet only)
Defence Science Representative (Bangkok)
Defence Central Library
Document Exchange Centre, DISB (18 copies)
Joint Intelligence Organisation
Librarian H Block, Victoria Barracks, Melbourne
Director General—Army Development (NSO) (4 copies)

(1 copy)

Aeronautical Research Laboratories

Director
Library
Superintendent - Aero Propulsion
Divisional File - Aero Propulsion
Author: P. D. McFadden

Materials Research Laboratories

Director/Library

Defence Research Centre

Library

RAN Research Laboratory

Library

Navy Office

Navy Scientific Adviser
RAN Aircraft Maintenance and Flight Trials Unit
Directorate of Naval Aircraft Engineering
Directorate of Naval Aviation Policy
Superintendent, Aircraft Maintenance and Repair

Army Office

Scientific Adviser—Army
Director of Aviation—Army
Royal Military College Library
US Army Research, Development and Standardisation Group

Air Force Office

Air Force Scientific Adviser
Aircraft Research and Development Unit
Scientific Flight Group
Library
Technical Division Library
Director General Aircraft Engineering—Air Force
Director General Operational Requirements—Air Force
HQ Operational Command (SMAINTSO)
HQ Support Command (SLENGO)
RAAF Academy, Point Cook

Government Aircraft Factories

Manager
Library

DEPARTMENT OF AVIATION

Library
Flight Standards Division

STATUTORY AND STATE AUTHORITIES AND INDUSTRY

Trans-Australia Airlines, Library
Qantas Airways Limited
Ansett Airlines of Australia, Library
Commonwealth Aircraft Corporation, Library
Hawker de Havilland Aust. Pty. Ltd., Bankstown, Library

CANADA

International Civil Aviation Organization, Library
NRC
Aeronautical & Mechanical Engineering Library
Division of Mechanical Engineering, Director

Universities and Colleges

Toronto Institute for Aerospace Studies

FRANCE

ONERA, Library

INDIA

Defence Ministry, Aero Development Establishment, Library
Hindustan Aeronautics Ltd., Library
National Aeronautical Laboratory, Information Centre

JAPAN

National Aerospace Laboratory
National Research Institute for Metals, Fatigue Testing Division
Institute of Space and Astronautical Science, Library

NETHERLANDS

National Aerospace Laboratory (NLR), Library

NEW ZEALAND

Defence Scientific Establishment, Library
RNZAF, Vice Consul (Defence Liaison)
Transport Ministry, Airworthiness Branch, Library

SWEDEN

Aeronautical Research Institute, Library
Swedish National Defense Research Institute (FOA)

SWITZERLAND

Armament Technology and Procurement Group

UNITED KINGDOM

Ministry of Defence, Research, Materials and Collaboration
CAARC, Secretary
Royal Aircraft Establishment
Bedford, Library
Commonwealth Air Transport Council Secretariat
Admiralty Research Establishment
St Leonard's Hill, Superintendent
Naval Aircraft Materials Laboratory, Library
National Physical Laboratory, Library
National Engineering Laboratory, Library
British Library, Lending Division
Aircraft Research Association, Library
Westland Helicopters Ltd., Library
Stewart-Hughes Ltd., Southampton

Universities and Colleges

Bristol	Engineering Library
Cambridge	Library, Engineering Department
	Dr J. D. Smith, Engineering Department
Southampton	Library

UNITED STATES OF AMERICA

NASA Scientific and Technical Information Facility
Nondestructive Testing Information Analysis Center

SPARES (20 copies)

TOTAL (120 copies)

Department of Defence
DOCUMENT CONTROL DATA

1 a. AR No AR 004 049	1 b. Establishment No ARL AERO PROP R 169	2. Document Date September 1985	3. Task No. DST 82 051
4. Title ANALYSIS OF THE VIBRATION OF THE INPUT BEVEL PINION IN RAN WESSEX HELICOPTER MAIN ROTOR GEARBOX WAK143 PRIOR TO FAILURE		5. Security a. document Unclassified b. title c. abstract U. U.	6. No. Pages 26 7. No. Refs 29
8. Author(s) P. D. McFADDEN		9. Downgrading Instructions	
10. Corporate Author and Address Aeronautical Research Laboratories P.O. Box 4331, Melbourne, Vic., 3001		11. Authority (as appropriate) a. Sponsor c. Downgrading b. Security d. Approval	
12. Secondary Distribution (of this document) Approved for public release Overseas enquirers outside stated limitations should be referred through ASDIS, Defence Information Services Branch, Department of Defence, Campbell Park, CANBERRA, ACT, 2601.			
13. a. This document may be ANNOUNCED in catalogues and awareness services available to No limitations			
13. b. Citation for other purposes (i.e. casual announcement) may be (select) unrestricted (or) as for 13 a.			
14. Descriptors Vibration Gearboxes Helicopters Signal averaging Condition monitoring			15. COSATI Group 01030 13090 14020
16. Abstract <i>Following the crash of an RAN Wessex helicopter caused by the catastrophic fatigue failure of the input spiral bevel pinion in the main rotor gearbox, routine recordings of the gearbox vibration have been analyzed by ARL. It has been shown that conventional spectral analysis of the vibration is unable to give adequate indication of the presence of the fatigue crack but that an alternative technique of vibration analysis called signal averaging can give warning of the crack 42 hours before failure. Enhancement of the signal average using a computer enables detection of the crack as early as 103 hours before failure.</i>			

This page is to be used to record information which is required by the Establishment for its own use but which will not be added to the DISTIS data base unless specifically requested.

16. Abstract (Contd)		
17. Imprint Aeronautical Research Laboratories, Melbourne		
18. Document Series and Number Aero Propulsion Report 169	19. Cost Code 417425	20. Type of Report and Period Covered
21. Computer Programs Used		
22. Establishment File Ref(s)		

END

DATE
FILMED

12-86

DTI